EFFECT OF THE TEXTURAL AND ACID PROPERTIES OF MESOSTRUCTURED SILICA SUPPORTED Fe-W CATALYSTS IN THE HYDROCRACKING OF A MODEL COMPOUND OF HEAVY GAS OIL

JONATAN RICARDO RESTREPO GARCIA

UNIVERSIDAD INDUSTRIAL DE SANTANDER

FACULTAD DE INGENIERÍAS FISICOQUÍMICAS

ESCUELA DE INGENIERÍA QUÍMICA

CENTRO DE INVESTIGACIONES EN CATALÍSIS

MAESTRÍA EN INGENIERÍA QUÍMICA

BUCARAMANGA

2015

EFFECT OF THE TEXTURAL AND ACID PROPERTIES OF MESOSTRUCTURED SILICA SUPPORTED Fe-W CATALYSTS IN THE HYDROCRACKING OF A MODEL COMPOUND OF HEAVY GAS OIL

JONATAN RICARDO RESTREPO GARCIA

In partial fulfillment of the requirements for the degree of

Master of Science in the Department of Chemical Engineering

Prof. SONIA AZUCENA GIRALDO DUARTE

(Advisor)

UNIVERSIDAD INDUSTRIAL DE SANTANDER

FACULTAD DE INGENIERÍAS FISICOQUÍMICAS

ESCUELA DE INGENIERÍA QUÍMICA

CENTRO DE INVESTIGACIONES EN CATALÍSIS

MAESTRÍA EN INGENIERÍA QUÍMICA

BUCARAMANGA

2015

Dedicatoria

A Dios todo poderoso por su amor y misericordia, a mis Padres Martha y Ricardo por su amor y apoyo incondicional, porque su perseverancia, esfuerzo y diligencia me han inspirado a seguir adelante, me han brindado consuelo, gozo y la satisfacción del deber cumplido.

A mis hermanas Gineth y Mariana por darme la alegria de compartir con ellas mis victorias y mis fracasos, por siempre estar ahí.

A mi amigo Sebastián por su ejemplo, paciencia y buena voluntad.

A todos mis compañeros de laboratorio por su valiosa ayuda y apoyo.

AGRADECIMIENTOS

A nuestra directora del Centro de Investigaciones en Catálisis CICAT, Prof. Sonia A. Giraldo Duarte por darme la oportunidad de hacer parte de la familia del CICAT, su apoyo, diligencia, paciencia y buena voluntad.

A los profesores, Víctor G. Baldovino Medrano y Luz Marina Ballesteros Rueda por su asesoría y orientación.

A Departamento Administrativo de Ciencia Tecnología e Innovación COLCIENCIAS por el apoyo suministrado en la realización de esta investigación mediante la beca de “Jóvenes Investigadores 2012”

A la Vicerrectoría de Investigación y Extensión VIE-UIS por el apoyo brindado en la realización de esta investigación en el marco del proyecto de financiación interna código 1329

A mis evaluadores, Prof. Julio A. Pedraza y Prof. Viatcheslav V. Kafarov por dar el componente crítico a esta investigación, lo cual consolidó mi proceso de formación en lo personal y profesional.

A todos mis compañeros del Centro de Investigaciones en Catálisis CICAT por su asesoría, paciencia y apoyo en la realización de esta investigación.

CONTENT

LIST OF FIGURES

LIST OF TABLES

RESUMEN

TÍTULO: EFECTO DE LAS PROPIEDADES TEXTURALES Y ÁCIDAS DE CATALIZADORES Fe-W SOPORTADOS EN SILICE MESOESTRUCTURADA EN EL HIDROCRAQUEO DE UNA MOLÉCULA MODELO DE CRUDOS PESADOS*

AUTORES: Jonatan R. Restrepo Garcia **

PALABRAS CLAVE: Hidrocraqueo, tamices moleculares, catalizadores Fe-W, fenantreno, Al-SBA-15

DESCRIPCIÓN:

El hidrocraqueo de crudos presados requiere una alta mesoporosidad (mayor diámetro de poros) y una función ácida moderada en catalizadores soportados para tratar las moléculas voluminosas presentes en esta clase de materia prima y favorecer la producción de Destilados Medios (MD). Por lo tanto, se sintetizaron cinco clases de sílice mesoporosa basadas en SBA-15, se modificaron sus parámetros de síntesis y se aumentó su mesoporosidad. NH_4F y 1,3,5-trimethylbenzene (TMB) fueron usados para modificar el arreglo hexagonal del SBA-15 y con el objetivo de evaluar su influencia en reacciones de hidrocraqueo. Los materiales SBA-15 modificados con TMB mostraron mayores propiedades texturales (volumen y diámetro de poro) en comparación con las sílices modificadas con NH_4F y el SBA-15 puro. La acidez fue generada por un procedimiento de *"injertado químico"* post-síntesis para las relaciones molares Si/Al de 10, 25, y 40. Las fases activas sulfuradas Fe-W impregnadas sobre los soportes Al-SBA-15 y Al-SBA-TMB fueron probadas en la reacción de hidrocraqueo de fenantreno. Se observó que todos los catalizadores químicamente injertados con aluminio fueron selectivos a un compuesto de ruptura de anillo aromático (trans-stilben) asociado con acidez tipo Brönsted, como fue evidenciado con los resultados de ^{27} Al MAS NMR, este compuesto no fue obtenido al evaluar con el catalizador comercial NiMo/γ-Al_2O_3 cuya selectividad fue exclusiva a compuestos parcialmente hidrogenados.

* Tesis de Maestría

** Facultad de Ingenierías Físico-Químicas. Escuela de Ingeniería Química. Director: Sonia A. Giraldo.

ABSTRACT

TITLE: EFFECT OF THE TEXTURAL AND ACID PROPERTIES OF MESOSTRUCTURED SILICA SUPPORTED Fe-W CATALYSTS IN THE HYDROCRACKING OF A MODEL COMPOUND OF HEAVY GAS OIL*

AUTHORS: Jonatan R. Restrepo Garcia **

KEYWORDS: Hydrocracking, molecular sieves, Fe-W catalysts, phenanthrene, Al-SBA-15

DESCRIPTION:

Heavy Oil hydrocracking requires an enhanced mesoporosity (higher pore diameters) and a moderate acid function (mild acidity) on supported catalysts to treat the bulky molecules presented in this kind of feedstock and to yield middle distillates (MD). Therefore, five different kinds of mesoporous silica based on SBA-15 were synthesized by modifying its synthesis parameters aiming at enhancing mesoporosity. NH_4F and 1,3,5-trimethylbenzene (TMB) were used to modify the mesostructured arrangement in SBA-15 and also with the purpose of evaluating their influence in hydrocracking reactions. TMB modified SBA-15 materials exhibited the highest textural properties (pore volume and pore diameter) in comparison to NH_4F modified silica and pristine SBA-15 silica. Acidity was incorporated in a post-synthesis *"grafting procedure"* for Si/Al molar ratios of 10, 25, and 40. Sulfided Fe-W active phases were impregnated on Al-SBA-15 and Al-SBA-TMB supports and those were tested in the hydrocracking reaction of phenanthrene. It was observed that for all chemically grafted with Al catalysts were selective to an aromatic ring rupture compound (trans-stilben) associated with Brönsted acidity as shown in the results of the spectra of ^{27} Al MAS NMR, this compound was not evidenced by comparing with the commercial catalyst Ni-Mo/γ-Al_2O_3, which selectivity tended to partially hydrogenated compounds exclusively.

* Master Thesis

** Physical and Chemical Engineering Faculty. Chemical Engineering School. Advisor: Sonia A. Giraldo.

INTRODUCTION

The increase in the demand of Middle Distillates (MD) production by refining processes of heavy oils has recently turned the focus of researchers worldwide [1-4]. It is due to the difficulty in processing bulky molecules presented in this kind of feedstock with conventional catalysts, that it has been necessary developing new kinds of materials, which used as catalytic support may overcome diffusional limitations related to pore size in such catalysts[5-7].

Materials research during the last decades has demonstrated that it is possible to synthesize and modify silica based materials such as MCM-41 (Mobil Composition of Matter Nº 41), SBA-15 (Santa Barbara Amorphous Nº 5), and MCF (Mesocellular Foam) in order to use them as support for heavy oil upgrading catalysts [8-11]. Particular attention has been shifted to the SBA-15 type mesoporous silica, which possesses a wide pore volume, a narrow pore size distribution, and better hydrothermal stability compared to MCM-41 silica [12]. Therefore, using this material as support for hydrocracking (HCK) catalysts results in an interesting and challenging alternative to be studied and applied in hydro conversion processes, as it has been previously stated [12-14].SBA-15 mesoporous silica is formed by a hexagonal array of tubular and uniform cylindrical channels, which is obtained when triblock copolymers are used in strong acid media. This copolymer acts as surfactant and template to obtain the ordering pattern [10, 15, 16]. Zhao *et al***.,** have also studied the use of micellar swelling agents to modify the textural and structural properties of the SBA-15 by expanding the pore diameter, and with that modification treating heavier molecules [14, 15]. It has been reported that the use of organic co-solvents like 1,3,5-trimethylbenzene (TMB), hexane or n-butanol swells the pore size [8, 9, 16]. Moreover, it has been also attributed to small additions of inorganic salts the uniformity of the tubular channels. Thicker silica walls of the material is directly correlated with higher hydrothermal stability [16-18]. This feature makes SBA-15 a specific mesostructured material. However, the acidity of the support is low, due to

the neutral Si atoms conforming its structure, and for that, using only SBA-15 materials in heavy oil HCK does not direct the reaction to yield MD. In that sense, it has been incorporated different kind of metals like Al, Ti, Zr, Sn, which are promoters of the formation of Brönsted acid sites [19-21], and by varying Si/Al molar ratio in the synthesis of the materials, it leads to increase the acid function in those kind materials [22-25].

Aiming at enhancing textural and acid properties of SBA-15 based mesoporous silica, and preparing catalysts for HCK of heavy oil supported on these materials, it has been investigated the ordering and structural change among five kinds of mesoporous silica, formed using an amphiphilic triblock copolymer (Pluronic P123). SBA-15 based mesoporous silica were synthesized by the sol-gel method by two approaches, firstly by the addition of 0.10 and 0.15 g of NH_4F to the synthesis mixture before silica source incorporation. Secondly by varying the TMB:P123 mass ratio from 0.15 and 0.75 to swell pore diameter. Acidity enhancement was carried out by a post-synthesis grafting procedure changing the Si/Al molar ratio (10, 25, and 40).

Due to Fe-W supported catalysts have been less studied in the last decades [7, 26-29], studying reactivity over these kind of catalysts result interesting. Moreover, Fe promoted active phases are cheaper than Ni-W counterparts[30]. Therefore, we have prepared Fe-W catalysts supported on the highest pore size and pore volume synthesized SBA-15 based silica materials, which were tested in batch HCK reactions of phenanthrene, a model molecule for vacuum gas oil (VGO).

1. LITERATURE REVIEW

Catalysts in the process of refining heavy oil fractions have been widely studied in order to provide meaningful insight in the process of upgrading this kind of feedstock. Specifically, a hydrocracking catalyst is designed to favor the production of Middle Distillates [31, 32]. To this end, catalysts must be characterized of having an appropriate acid distribution and acid strength, and also a narrow pore size distribution, which is necessary to reduce the diffusional limitations effects by treating bulky molecules in heavy oil [33].

A lot of information about hydrocracking reaction is found widely in open access literature, the main differences are based upon the kind of catalytic support used in those kind of catalysts, and their modifications to enhance a specific function (hydrogenation and acidity) on the surface of the catalyst [5]. The main contributions in the field of synthesis and characterization of promising materials for hydro processing are found in the family of mesoporous silica like MCM-41, SBA-15 (specific surface area between 600 and 1000 m^2 g^{-1}), and MCF[11, 22, 34, 35]. For their industrial application, these materials need to be modified by a hydrothermal treating by increasing the synthesis temperature between 308 and 353 K in the Sol-Gel method, this increase in temperature during the aging procedure favors the formation of larger pore sizes[36]. On the other hand, hydrothermal stability can be reinforced by the incorporation of Al atoms within its framework, this incorporation does not only promote the stability of silica materials at high temperatures, and it also promotes the formation of Brönsted acid sites for the modified Al-SBA-15[29]. These modifications also change the activity and selectivity, therefore, it is essential adequately selecting the synthesis conditions to fulfill the main purpose of hydrocracking reactions[37].

Mesostructured silica SBA-15 type is a formed by a 2-D hexagonal arrangement of uniform and tubular channels with space group *p6mm*, tunable pore sizes within 5-

30 nm, and a narrow pore size distribution; this kind of silica was introduced by Zhao *et al.*, by a Sol-Gel synthesis procedure, using the triblock copolymer P123 as structural direction agent and surfactant in acid media conditions[15]. The use of amphiphilic triblock copolymers (hydrophobic and hydrophilic chains) to direct the formation of silica particles around the micelles has yielded in the preparation of well-developed mesoporous particles of SBA-15 and by adding organic molecules as co-solvents, the pore size has been increased; thus, this mesoporous materials has received most of the attention, since its applicability to improve catalytic activity in reactions, which require the conversion of bulky molecules, such as the vacuum gas oils (VGO) and others heavy oil fractions[7]. However, in comparison to conventional microporous zeolites, SBA-15 lacks of moderate acidity and high temperature stability, which is mainly attributed to its silicon framework[21]. Those drawbacks limit its application at industrial scale, especially, chemical reactions that involves treating at high temperatures above 573 K such as hydro processing reactions like hydrodesulphurization (HDS), hydrodenitrogenation (HDN), hydrodemetallation (HDM), and hydrocracking (HCK), among others. In particular, HCK reaction requires active acid sites, strong enough (moderate acidity) to crack the bulky molecules in lower molecular weight ones, Diesel fractions and gasoline [4, 38]. Hence, doping SBA-15 with different metallic ions (Al, Ti, Zr) has caught researcher's attention. This heteroatom incorporation with lower valences than silicon generates negative charges on the surface of the material, which are compensated by H^+ and subsequently promotes the formation of acid sites[19, 26, 39]. During the last decades, partial replacement of Si^{4+} ions by Al^{3+} ions has been more studied as a result of the moderate acidity attained without changing significantly the mesostructured pattern of SBA-15 [29]. Al incorporation has been successfully achieved by direct or post-synthesis methods either by adding the Al precursor during the synthesis of the SBA-15 silica or by chemical grafting procedures [28, 40]. Al incorporation on SBA-15 framework is directly correlated to Brönsted acid sites and the improvement of its hydrothermal stability; Brönsted acid sites are formed as a result of the terminal silanol groups in the vicinity of an aluminum atom or binding

hydroxyl groups[41]. Conversely, direct Al incorporation methods is a difficult process to be achieved during the synthesis of SBA-15, since under acid media conditions (pH<1), Al does only exist in its oxidized form; this incorporation also disfavors the textural properties, specifically pore size[42].

Soni *et al*., proposed the *in situ* incorporation of Ti by using titanium isopropoxide, which exhibited a better dispersion of octahedral Ni and Mo species on the surface of the Ti-SBA-15 than on pristine SBA-15, which was correlated to high activity in HDS and HDN reactions with heavy oil at 8 MPa with a range of temperature between 603 to 643 K [10]. Zhang *et al.*, studied the effect of acidity and textural properties of Ni-W catalysts supported on a bi-modal material composed of USY zeolite and the hydrothermally synthesized Al-SBA-15, HCK reactions of model compounds of heavy oil such as cumene, and 1,3,5-trisiopropylbenzene were tested to elucidate the reaction mechanism, later those catalysts were tested with heavy oil. The strong acidity related to USY zeolite was evidenced by the rupture of the model compounds, and the effect of Al-SBA-15 porosity enhanced the activity with heavy oil. The effect of Al-SBA-15 acidity was not clearly evidenced since USY zeolites are more acid than Al-SBA-15 [14]. Li *et al.*, proposed the post-synthesis incorporation of Al on SBA-15 by aluminum nitrate, which was accomplished by the pH modification with ammonium hydroxide in the synthesis of Al-SBA-15, then, to analyze the effect of this modification HDS test with dibenzothiophene (DBT) were performed with Ni-W (2 wt. % and 23 wt.% respectively) active phases supported on Al-SBA-15. With this approach, the formation of acid sites was increased at expenses of specific surface area, the formation of extra framework aluminum species also increased as the same rate tetrahedral aluminum species formation[43].

Zhiping *et al.*, synthesized Ni-W/SBA-15 catalysts, which were tested in HDN and HDS batch reactions with heavy oil fractions, experiments were tested at 5 MPa of H_2 partial pressure and 673 K. It was concluded that the method of synthesis of

catalysts had a great influence on the activity of the reactions depending on the Ni/W molar ratio on the surface of the SBA-15 supports [23].

Boahene *et al.*, studied the effect of different pore sizes Fe-W/SBA-15 catalysts in the hydro treating reactions (HDN and HDS) of Athabasca bitumen, larger pore sizes were obtained by adding n-hexane as a micellar swelling agent. Catalysts with pore diameter larger than 13 nm exhibited the lowest activity. Nonetheless, Fe-W hydrogenation function could be tested in hydro treating reactions [8, 9]. Similarly Mouli et al., synthesized Al-SBA-15 by adding the aluminum precursor during the synthesis of SBA-15 with larger pore size by the addition of n-hexane without collapse of the structure. This support was used to prepare Ni-Mo catalysts, the activity of HDS reaction was more promoted by this catalyst than HDN activity by testing oil sands[10].

In the field of HCK reactions Byambayav *et al.*, synthesized and tested Fe/SBA-15 and Ni/SBA-15 (10 wt.% of metal content) catalysts on the hydrocracking of asphaltenes derived of heavy oil at 5 MPa and 573 K. A 70% of conversion was found for the Fe loaded catalysts, thus, Fe influences the hydrocracking mechanism[12, 44]. The effect of Al incorporation on the Brönsted surface acidity of Al/SBA-15 was studied in detail by Koekkoek *et al.*, using solid state ^{27}Al MAS NMR analyses and a free of water method of synthesis to favor the dispersion of Al on the surface of SBA-15. The highest dispersion of Al was found for Si/Al molar ratios higher than 10, tetrahedral aluminum species were formed predominantly with low content of Al. In terms of acidity IR spectroscopy revealed that the intrinsic acidity of Al/SBA-15 is comparable to zeolites and amorphous alumino-silicates (ASA). This, it is ratified that the acid sites distribution governs the differences in acidity in alumino-silicates[45].

Jaroszeweska *et al.*, addressed the performance of noble metal (Pt) catalysts supported on Al-SBA-15 by testing different loads of Pt catalysts on the hydrocracking reaction of decalin an 1-methylnaphtalene at 623 K at a fixed bed

reactor. Three Al precursors were employed (aluminum isopropoxide, aluminum nitrate and aluminum sulphate), 1-methylnaphtalene conversion was not directly promoted by the source of Al during the synthesis procedures, this was promoted by the content of Pt on the catalysts (0.5, 2.5, and 4.5 wt. %). Metallic phase dispersion was highly favored by the lower content of Pt on Al-SBA-15 supports [46, 47].

Based on the previous literature review given, it can be inferred that the effects of Al incorporation on the selectivity and activity of hydrocracking reactions is not well understood, most of the research focused on this support was conducted with heavy oil fractions, which does not allow to conclude about the mechanism of hydrocracking reaction on Al-SBA-15 supported catalysts. Therefore, using model compounds of heavy oil fractions may open a new insight of the catalytic phenomenon thereof. Moreover, testing catalysts with less expensive active phases such a Fe-W metallic phases turns the focus of catalysts for heavy oil upgrading.

2. EXPERIMENTAL

2.1 MESOPOROUS SILICA SYNTHESIS

Five kinds of SBA-15 based mesoporous silica were prepared with different pore sizes, using Pluronic P123 ($EO_{20}PO_{70}EO_{20}$, M_{av}=5800, Aldrich) as structural *direction* agent (SDA), Tetraethylortosilicate (TEOS, 98% Aldrich) as silica source in strong acid media conditions (pH<1), and modifying procedures previously reported in literature by two procedures[8, 15, 17]. The first procedure consisted in using NH_4F (99% Aldrich) to favor ordaining on accordance with the following nominal molar ratio: 1.0 TEOS: 0.0169 P123: 4.42HCl:186 H_2O, the second procedure involved the addition of TMB at the same precursor's nominal ratio.

In a SBA-15 typical synthesis 10 g of P123 were completely dissolved in 1.3 M HCl (37 vol. %, Merck) aqueous solution under stirring (500 rpm). Then, 24 mL of TEOS was added drop by drop and was kept under agitation for 1 h. Subsequently the temperature was increased from room temperature to 311 K and kept during 24 h. The milky suspension thus obtained was transferred into a 500 mL PTFE closed bottle, where in static conditions and under autogenous pressure the hydrothermal treatment at 403 K was performed for 24 h in a muffle furnace. The solid product was filtered and washed with abundant deionized water, and kept static for 24 h at room temperature. Then the material was calcined under dry air flow (100 mL/min) at 773 K during 6 h with a heating rate of 2°C/min to remove the template.

SBA-F(0.10) and SBA-F(0.15) samples were synthesized by adding 0.10 g and 0.15 g of NH_4F to the synthesis mixture before TEOS incorporation, SBA-TMB(0.15) and SBA-TMB(0.75) were obtained adding the required amount of TMB to get TMB: P123 mass ratios of 0.15 and 0.75 before dropwise TEOS incorporation and kept until homogenization for 1 h. The other steps remained the same for SBA-15 preparation.

2.2 ALUMINUM INCORPORATION

Surface acidity of the supports was obtained by an Al post-synthesis *grafting procedure* [28]. The powdered samples (5 g) were grafted under constant agitation (500 rpm) for 18 h in a 0.02 M ethanol (Merck, 98%) solution of aluminum isopropoxide ($C_9H_{21}AlO_3$, Merck 98%) for Si/Al molar ratios of 10, 25 and 40. Basic media was controlled by adding drop by drop an aqueous solution of NH_4OH (28 vol. %, Aldrich, 98%) to get a pH in the range of 9.0-9.5. The grafted materials were filtered and washed with ethanol to remove residues of aluminum precursor. Then, those materials were calcined under dry air (100 mL/min) at 773 K for 6 h. Al-modified materials were labeled Al(x)-SBA-15 and Al(x)-SBA-TMB(0.75) , where “x” indicates the Si/Al molar ratio.

2.3 CATALYSTS PREPARATION

Fe-W catalysts supported on γ-Al_2O_3 (*Protocatalyse*), Al(x)-SBA-15 and Al(x)-SBA-TMB(0.75) were prepared by the successive incipient wetness impregnation method. $Fe(NO_3)_3.9H_2O$ (98%, Aldrich) and $(NH_4)_6H_2W_{12}O_{40}.H_2O$ (98%, Aldrich) aqueous solutions (30 % in excess of the required amount to fill pore volume of catalysts) were used as Fe and W precursors. After each impregnation the catalysts were dried at 393 K during 12 h with a heating rate of 2ºC/min, and then calcined under dry air flow (100 mL/min) at 773 K during 6 h at the same heating rate. Metallic oxides loading was Fe_2O_3 (3 wt. %) and WO_3 (15 wt. %). Non sulfided catalysts were labeled as Fe-W/Al(x)-SBA-15 and Fe-W/Al(x)-SBA-TMB(0.75). All catalysts were sieved to get a particles size range between 25 µm and 75 µm.

2.4 CHARACTERIZATION OF SUPPORTS AND CATALYSTS

2.4.1 Textural characteristics

All samples (0.2 g) were degassed at 393.15 K for 12 h before the analysis. Then the specific surface area was determined based on Brunauer, Emmett and Teller

(BET) theory for all supports and catalysts prepared by measuring adsorption-desorption isotherms of N_2 at 77 K in a 3FLEX *Micromeritics* apparatus.

BET specific surface area was computed within the linear relative pressures range of 0.04 to 0.24 according to IUPAC recommendation for this kind of measurements[48].Total pores volumes were calculated from the amount of nitrogen adsorbed at a relative pressure (P/P_0) of 0.9. Pore volumes and diameters were estimated by N_2-DFT model incorporated in the apparatus software.

2.4.2 XRD patterns

Catalysts and supports samples (0.2 g) were powdered in an agate mortar until a particle size of 38 µm. Measurements were carried out in a Bruker Advance diffractometer with Da Vinci geometry using Ni-filtered CuKα1 radiation (40 kV, 30 mA). Low angle analyses were performed with the purpose of identifying changes in the material ordering pattern. The 2θ degrees range was scanned between 0.5° and 8° with a step size of 0.01526° and a counting time of 0.4 s per step. Qualitative analysis of the registered peaks was carried out by comparing with the diffraction profile reported in the database PDF-4+ ICDD (SiO_2-00-058-0344). Wide angle analyses were performed for all catalysts in order to confirm the formation of the respective oxidized species of the metals incorporated. The 2θ degrees range was scanned between 10° and 80°.

2.4.3 Scanning-electron-microscopy (SEM)

Scanning electron microscopy was employed to obtain morphological observations on the surface of the obtained silica materials, and to identify a change in the shape of the SBA-15 particles with the modified parameters. The procedure was performed in a scanning electron microscopy FEI Quanta 650 FEG operating with an electron voltage of 4.00 kV. The study was carried out with magnifications of 20 µm, 3 µm, and 500 nm; depending on the size of the particle to be observed.

2.4.4 ^{27}Al MAS NMR solid measurements

^{27} Al MAS NMR experiment in the solid state was conducted to B_0 = 9.4 T on a Bruker ADVANCE 400 WB III apparatus. The resonance frequency corresponding to ^{27}Al was 104.3 MHz. All the grafted supports labeled as Al(x)-SBA-15 and Al(x)-SBA-TMB(0.75) were analyzed. The MestReNova 9.0 software was used to compute the content of the incorporated aluminum species by a Gaussian integration of their respective peaks.

2.4.5 Proton affinity distributions (PAD)

The proton affinity of the materials was measured by potentiometric titration in a TitroLine 7000 (SI Analytics) titrator. Each sample of catalysts and supports were sieved to get a particle size less than 75 µm [28]. 0.05 g of the samples were added to a 0.01 N aqueous solution of $NaNO_3$ (99.5% Merck). The suspension was homogenized by magnetic stirring for 30 min. For titration in the basic pH interval, it was used as titrating agent an 0.1M aqueous solution of NaOH (Merck 99%), which was added to 0.03 mL each 90 s until a pH of 10 was reached. Similarly titration was performed in the acidic pH range for a fresh sample with HCl (37 vol. %, Merck) 0.1 M until a pH of 3. The pH changes were measured in terms of the volume (basic or acidic) of the solution added. The acquired data were used to construct a proton consumption function (f(logk)) as a function of pH by a proton balance [49-51].

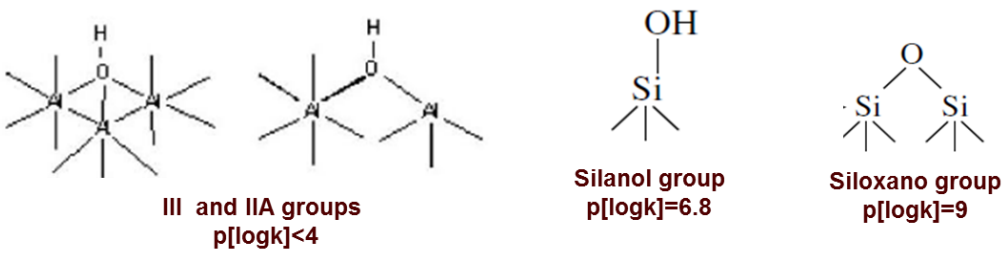

Fig. 1. Alumina and silica surface groups presented in aluminosilicates

Based on the acid sites distribution for alumina supports proposed by Knözinger and Ratnasamy, and depicted in Fig.1, the proton consumption was computed for all the supports and catalysts prepared. Depending on the OH groups configuration on the surface of alumina different acid sites are identified [51]. Quantification of OH groups was performed by a Gaussian deconvolution of the obtained peaks from proton consumption curves. To this end, the OriginPro 8.5.1 software was used. The area under each curve indicates the amount of acid sites [mmol $H^+.g^{-1}$ cat] present in the samples. Trends in the quantification of the OH groups derived from the PADs have mostly a qualitative value, being valid only for comparing the series of catalysts prepared in this study.

2.5 CATALYTIC EVALUATION

2.5.1 Preliminary paraffins hydrocracking tests

A set of preliminary reactions were conducted in a 570 ml stainless steel batch reactor (Parr) to understand the effect of Fe-W active phases in the hydrocracking of a paraffin. To this end, two model molecules were tested separately by adding into the reactor a 250 mL liquid mixture composed by a of 4 wt. % of: firstly a linear hydrocarbon, n-hexadecane (Aldrich, 98%), and secondly a multi-branched hydrocarbon, 2,6,10,14-tetramethylpentadecane (Aldrich 98%), using as solvent n-heptane (Merck, 98%) in both cases.

Before the reaction, Fe-W/Al(10)-SBA-TMB(0.75) catalyst (1 g) was activated (sulfidation process) *ex-situ* under a flow of 100 ml min^{-1} of a mixture of H_2S/H_2 (15/85 vol. %) at 673 K for 4 h. The reaction conditions were 623 K and PH_2=2.2 MPa based upon the industrial hydrocracking reaction conditions [3].

Further description of the operational conditions and samples analysis are described in detail in the following section (section 3.5.2)

2.5.2 Phenanthrene hydrocracking tests

Sulfided catalysts were tested at the same conditions of the preliminary reactions, the liquid mixture occupied 250 ml and was prepared using 4 wt. % phenanthrene (Aldrich, 98%), 94 wt. % n-heptane (Merck, 98%) as solvent and 2 wt. % n-hexadecane (Aldrich, 98%) as an internal standard for chromatographic analyses.

The reactor was hermetically sealed after the addition of the presulfided catalyst to the liquid mixture. H_2 (PH_2=2.2 MPa) was added and the temperature was increased under agitation (1000 rpm) with a heating rate of 2ºC/min until 350ºC, the final pressure was 11 MPa. In this conditions of pressure and temperature, it was taken the first liquid sample, which, corresponds to the initial time (zero) of reaction. The following samples were taken each 15 min for the first hour, each 30 min for the second hour, and each hour for the last two hours. It was measured the samples and purges volumes in each interval. Liquid products of reaction were analyzed by GC, using a GC-HP 6890, equipped with a FID detector and a HP-1 (100mx0.25mmx0.5 µm) column. Products were identified by GC-MS, using a column HP-5 (30mx0.25mmx0.25µm), and by comparing the mass spectra of the liquid products obtained with the data basis W.8.1 (Data Analysis Chemstation Agilent Technologies).

Commercial Catalyst Ni-Mo/γ-Al_2O_3 *Protocatalyse* was also tested for comparison purposes.

2.6 EXPRESSION OF RESULTS

2.6.1 Catalysts Activity

Hydrocracking reaction initial rate can be expressed to a first order kinetic due to the high excess of hydrogen, and also because the expected behavior is like elementary reactions rather than multiple steps reactions [2, 6, 10, 12, 16, 23]. Therefore, initial reaction rates were computed by conversion data of phenanthrene corresponding to t= 0 min until t=60 min. It was used the pseudo-first order equation (1) proposed by

Gevert et al. [52], which, incorporates a correction factor due to purges and samples volumes, as depicted with equation (2).

$$-ln\left(\frac{C_i}{C_0}\right) = k_{Phen} W f\left({}^{t}/_{V}\right) \qquad (1)$$

$$f\left({}^{t}/_{V}\right) = \sum_{i=1}^{n} \frac{t_i - t_{i-1}}{V_{i-1}} \qquad (2)$$

Where: C_i, C_0 [g/mL] correspond to phenanthrene concentration in each *t* time when i samples are taken and in *t=0* min of reaction, *W* [g] is the weight of the catalyst, t_i, t_{i-1} [min] is the time until taking two consecutive samples, V_{i-1} [mL] is the remaining solution volume after taking the sample $i-1$.

2.6.2 Selectivity

Selectivity towards a specific product (9,10-dihydrophenanthrene, 1,2,3,4-tetrahidrophenanthrene, trans-stilben) was computed by equation 3.

$$y_i = \frac{mol_i}{mol_{Phen-reaction}} \qquad (3)$$

Where mol_i: are the i product moles (phenanthrene, trans-stilben, 9,10-dihydrophenanthrene, 1,2,3,4-tetrahydrophenanthrene) and $mol_{Phen-reaction}$: are the moles of phenanthrene consumed during the reaction.

3 RESULTS

3.1 CHARACTERIZATION OF CATALYSTS AND SUPPORTS

3.1.1 Textural characteristics

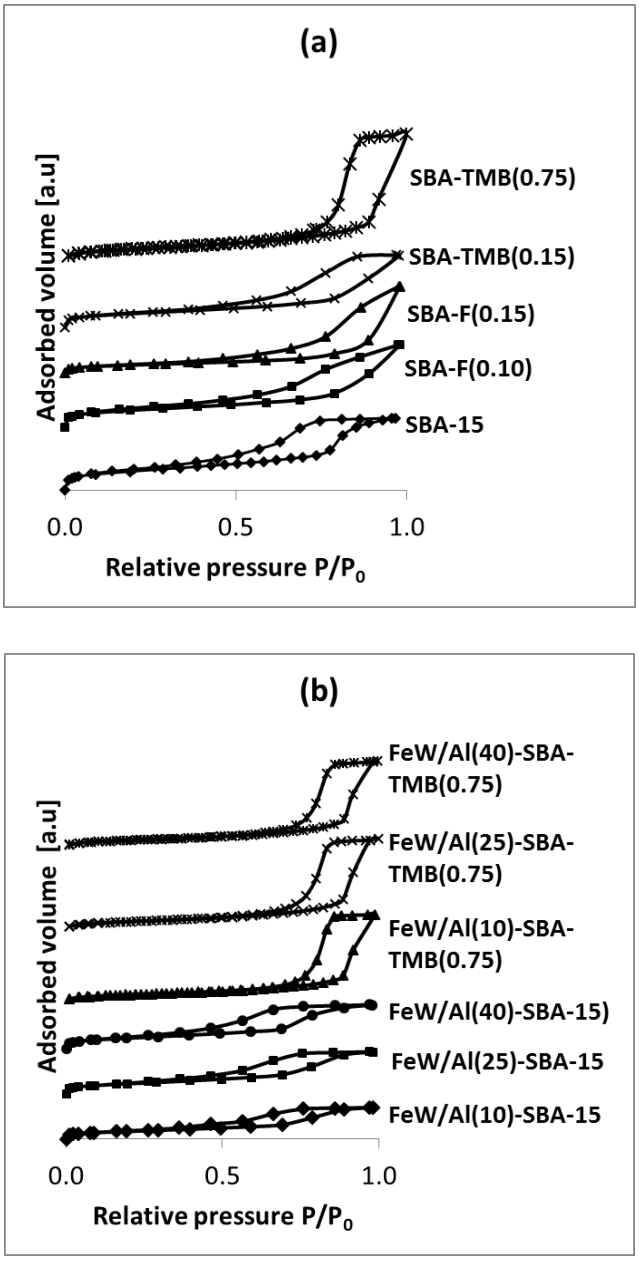

Fig. 2. N_2 adsorption-desorption isotherms, (a) silica materials, (b) catalysts

Fig. 2. shows the N_2 adsorption-desorption isotherms for all catalysts and silica materials synthesized, which exhibit a type IV isotherm according to the IUPAC classification, which characterizes mesoporous materials[48].

A wider H1 type hysteresis loop is found for the labeled samples SBA-15, SBA-TMB(0.15) and SBA-TMB(0.75), according to Fig. 2 (a). This is characteristic of uniform pores with defined geometry, generally tubular. The adsorption and desorption curves tend to be parallel between them at high relative pressures [53].

The SBA-F(0.10) and SBA-F(0.15) samples reveal a narrower and not parallel H1 type hysteresis loop at high relative pressures, which is characteristic of non-uniform pores. The change in the shape of the loop indicates a change in the pores geometry, indirectly showing the effect in the pore ordering, when adding inorganic salts in the amounts used. However, mesoporosity was preserved in all cases and confirmed by the presence of the hysteresis loop for all samples.

Fig. 2 (b) shows that for all catalysts is presented a narrower hysteresis loop compared to SBA-15 and SBA-TMB(0.75) materials. This result indicates that there is a decrease in the adsorption capacity when metal phases and aluminum content are added.

Table 1 shows the change in the textural properties of materials. In all cases the specific surface area presented a decrease, which was more marked for the materials prepared with the addition of NH_4F and allows to establish the collapse of mesostructured SBA-15 ordering pattern.

An increase in the pore diameter and pore volume with an increase in TMB: P123 mass ratio, for SBA-TMB(0.15) and SBA-TMB(0.75) is evidenced, which ratifies the expanding effect of TMB as swelling agent. For SBA-F(0.10) and SBA-F(0.15) samples this increase in pore diameter became remarkable with a higher amount of NH_4F. However, by comparing SBA-F(0.15) with SBA-TMB(0.75), pore volume and BET area are higher for SBA-TMB(0.75) silica. Pore diameter is practically the same

than SBA-F(0.15). Therefore, the silica support which evidenced enhanced textural properties is the silica SBA-TMB(0.75), which is selected for catalysts preparation.

Compared to γ-Al_2O_3 all silica materials synthesized showed higher specific surface area, pore sizes and pore volumes.

Table1. Textural properties of non-activated catalysts and supports

Sample	P_V (cm^3/g)	S_{BET} (m^2/g)	P_D (nm)	C_{BET}
γ-Al_2O_3	0.62	203	12	83
SBA-15	1.51	901.5	6.4	109
SBA-F(0.10)	1.41	709.3	7.8	55
SBA-F(0.15)	1.48	396.3	18	29
SBA-TMB(0.15)	1.23	586.8	8.6	74
SBA-TMB(0.75)	2.16	727.9	17.2	166
Fe-W/Al(10)-SBA-15	0.54	316.8	6.6	64
Fe-W/Al(25)-SBA-15	0.72	416.0	6.9	75
Fe-W/Al(40)-SBA-15	0.76	442.8	6.8	60
Fe-W/Al(10)-SBA-TMB(0.75)	1.37	351.5	17.2	135
Fe-W/Al(25)-SBA-TMB(0.75)	1.56	392.8	17.2	132
Fe-W/Al(40)-SBA-TMB(0.75)	1.47	393.5	17.2	272

S_{BET}= specific surface area, P_V= pore volume, P_D pore diameter, C_{BET}= constant BET

Fig. 3 shows the pore size distribution for all mesoporous silica. A bi-modal pore size distribution (microporosity and mesoporosity) is attained, the development of micropores while expanding pores is more evident by the addition of TMB as swelling

agent in comparison to SBA-15 (Fig. 3 (a)). Gaussian and narrow pore sizes distributions were evidenced for SBA-15 and silica materials modified with TMB than the others modified with NH_4F, indicating uniformity in pore sizes for TMB modified silica materials.

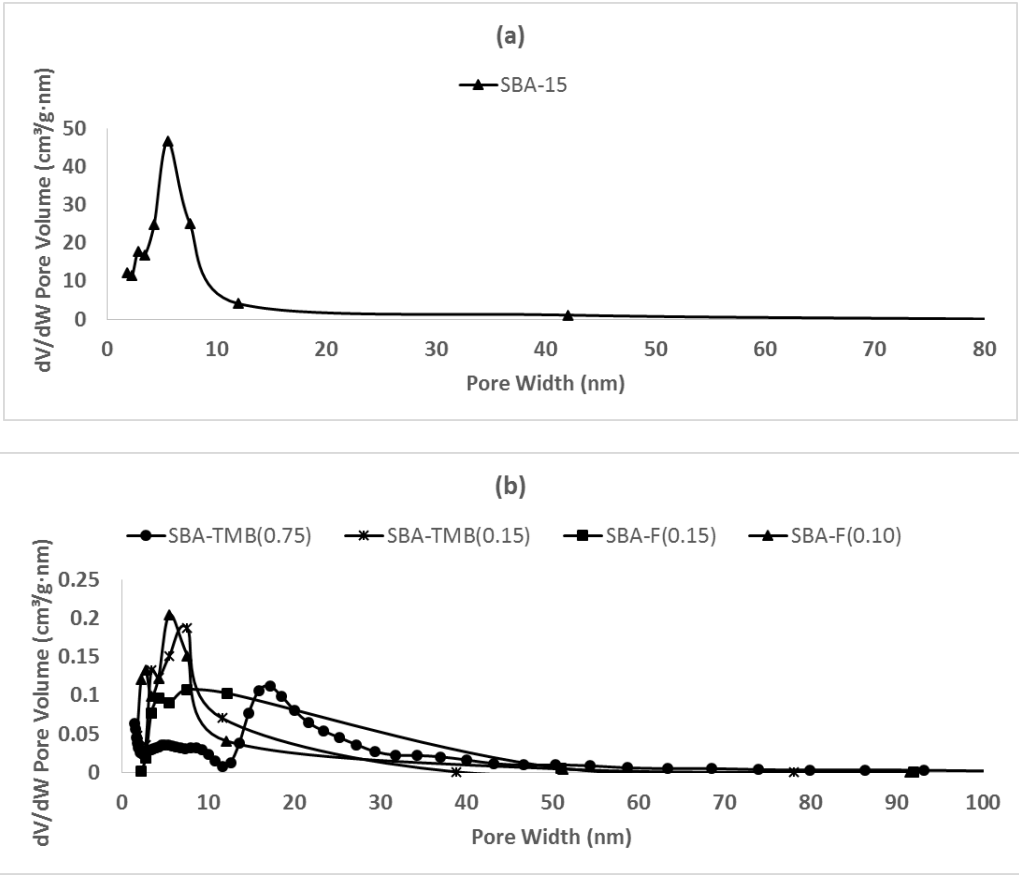

Fig. 3. Pore size distributions, (a) SBA-15, (b) Modified silica materials

Textural properties of the non-activated catalysts are shown in Table 1, there is a decrease in the specific surface area with a decrease in the Si/Al molar ratio, which is correlated with a narrow hysteresis loop in comparison with pristine SBA-15 and SBA-TMB(0.75) supports. Pore diameter reported values for Fe-W/Al(x)-SBA-TMB(0.75) catalysts remains constant. Therefore, no obstruction of pores is evidenced as a result of metals impregnation or aluminum content.

In terms of the changes of pore volume in the catalysts, it's shown a decrease in the pore volume with a decrease in the Si/Al molar ratio. It may be directly related with the higher amount of Al species for the Si/Al molar ratio of 10, and it's more evident for Al(x)-SBA-15 supported catalysts instead of Al(x)-SBA-TMB(0.75) supported catalysts, because of the higher pore volume Al(x)-SBA-TMB(0.75) possesses.

Constant C values reported established that BET method is adequately fitted for the determination of textural properties of the materials synthesized. All C values are within the range (C<300) of accuracy and physical meaning.

3.1.2 XRD patterns

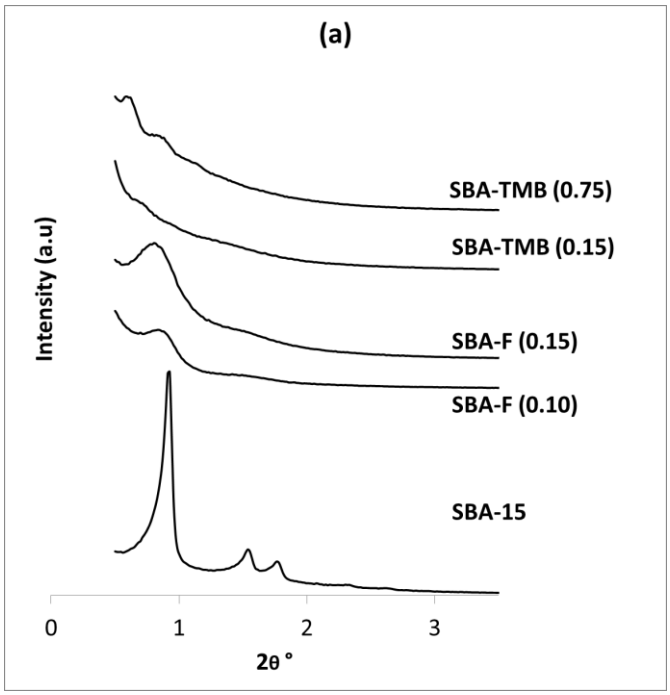

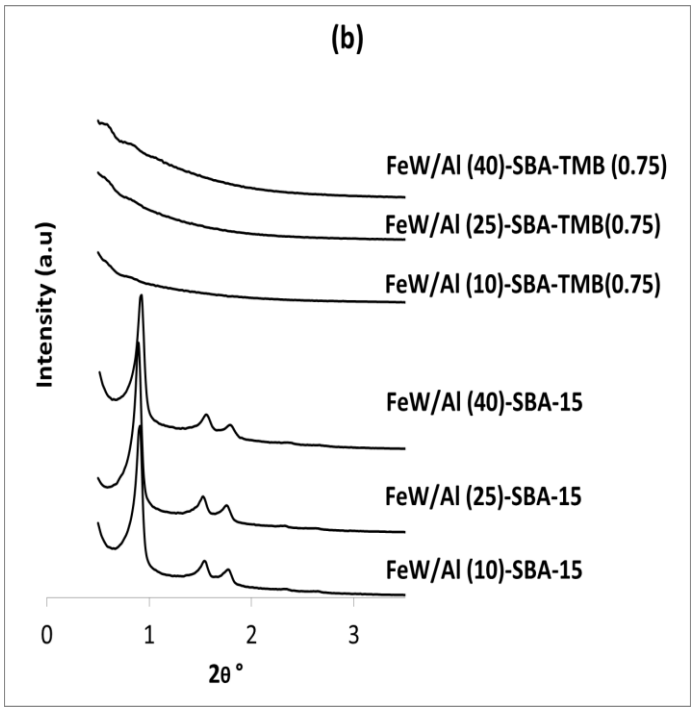

Fig. 4. Low Angle XRD patterns, (a) silica materials, (b) Non-activated catalysts

Fig.4. depicts low angle diffraction profiles, which show the reproduction in the synthesis of SBA-15 material, evidencing three identified peaks in 2θº of 0.9, 1.5 and 1.9, which are characteristic of the obtained hexagonal symmetry, with space group *p6mm*[15].

Fig 4. (a), shows for the modified materials SBA-F(0.10) and SBA-F(0.15), that only one peak is evident with less intensity than the SBA-15, and the disappearance of the peaks of the other planes. For TMB modified materials, a shift leftwards of the 3 peaks is observed for SBA-TMB(0.75), which unquestionably shows a change of the structure and rearrangement of the pores for the modified silica supports.

For catalysts prepared in Al(x)-SBA-15 not change is evident intensity and shape of the diffraction peaks according to Fig 4, (b). This is indicative that the addition of aluminum and metal phases on the surface of the catalyst retained SBA-15 low angle diffraction pattern and ordering.

For catalysts prepared on Al(x)-SBA-TMB(0.75) is possible to observe in Fig. 4 (b) a decrease in intensity of the three diffraction peaks. It is more evident for FeW/Al(10)-SBA-TMB(0.75) catalyst, which possess greater amount of aluminum content. Fe-W/Al(40) -SBA-TMB(0.75) catalyst showed almost the same diffraction pattern than SBA-TMB(0.75) support (Fig. 3 (a)). Based on the metal content is the same for all six catalysts, the change in the intensity is attributed to the aluminum content for the lower Si/Al molar ratio. Higher aluminum incorporation degraded the structure of Al(x)-SBA-TMB(0.75) supported catalysts.

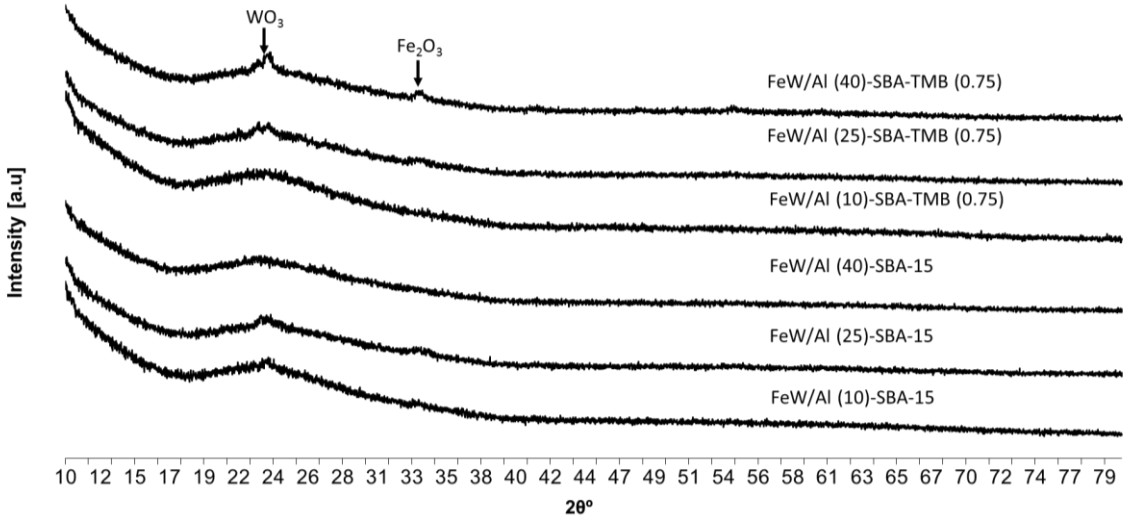

Fig. 5. Wide Angle XRD patterns for Fe-W/Al(x)-SBA-15 and Fe-W/ Al(x)-SBA-TMB(0.75) catalysts, x= Si/Al molar ratio

Fig. 5 shows the wide angle diffraction patterns for Fe-W/Al(x)-SBA-15 and Fe-W/Al(x)-SBA-TMB(0.75) catalysts. Fe-W/Al(x)-SBA-TMB(0.75) catalysts showed only the characteristic hump of SiO_2 material in the 2θº range centered between 19º and 27º [8]. The high surface area of silica support favors dispersion of the active phases, suggesting that either metals were homogeneously dispersed on the support or their compositions were below the detection limit of the X-ray signals. The absence of XRD signals in wide angle region indicates that the particle size of metals is below the coherence length of X-ray scattering. However in the case of Fe-W/Al(40)-SBA-TMB(0.75), it exhibited the same peak lift characteristic or silica-

based material. But a slight development of other two peaks is evidenced in 2θº of: 33.2 and 24.4, which are attributed and confirmed to oxidized species of the respective impregnated metals (Fe_2O_3 and WO_3). However, its least surface area and higher pore volume may have contributed to the formation of aggregates as detected by the X-ray (particle size >4 nm).

3.1.3 Scanning-electron-microscopy (SEM)

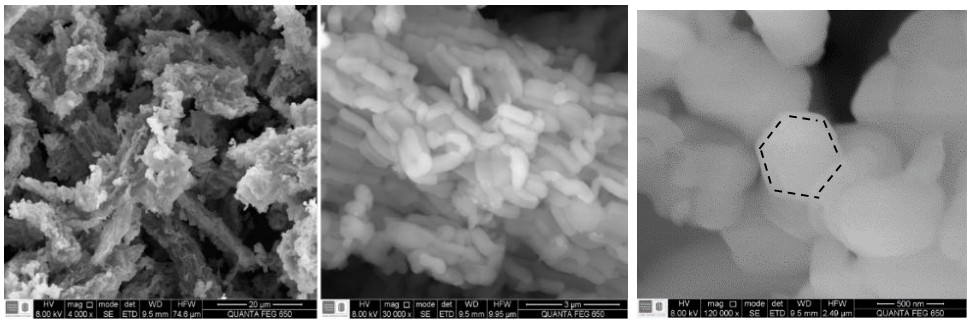

Fig. 6. SEM Images SBA-15

Fig. 6 shows the fibrous morphology of SBA-15 particles, result that ratifies the previously reported images for this kind of material [15], and for that indicates a reproduction of the synthesis of SBA-15 mesoporous silica. Fig. 5 also shows the fiber's hexagonal shape, which is characteristic for this type of material.

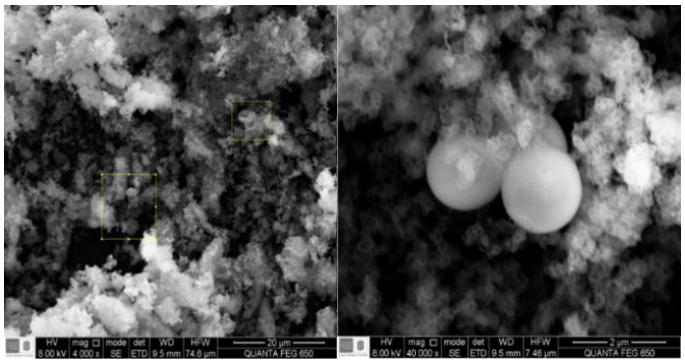

Fig. 7. SEM images of SBA-F(0.10)

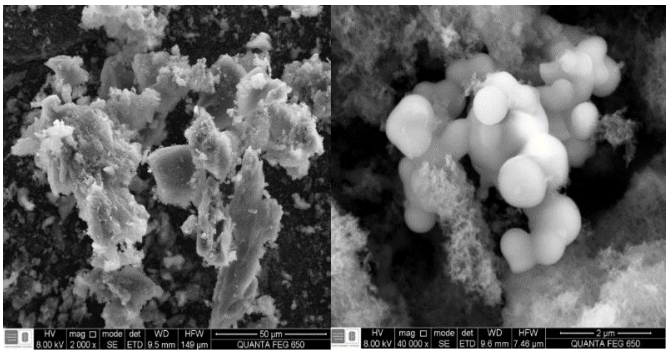

Fig. 8. SEM micrographs for SBA-F(0.15), spherical particles detailed

For samples labeled as SBA-F(0.10) and SBA-F(0.15) (Fig.7 and Fig.8), the amount of NH_4F added made it possible to increase the formation of spherical particles, however, that formation is not well developed and controlled with this approach, due to the effect in pH, which affects the strong acid media required for obtaining SBA-15 [15, 54]. Moreover, those spherical particles are specifically localized into amorphous silica. Therefore, most of the silica particles formed are result of the collapse of the structure due to the pores swelling. This occurs by either the basic change in the pH synthesis and by the interactions fluoride ions have with the hydrophobic chains in P123 dissolution. Then changing the shape of the micelles of the copolymer in the formation of well-developed silica particles as it has been previously stated by several authors [8, 9, 55].

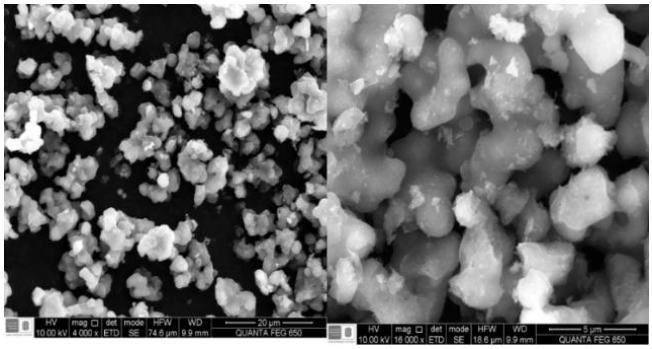

Fig. 9. SEM micrographs for SBA-TMB(0.15)

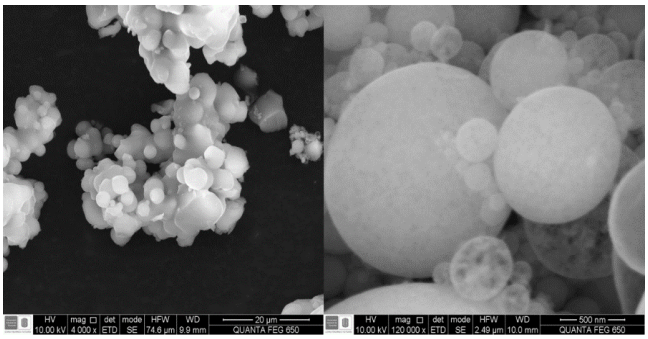

Fig. 10. SEM micrographs for SBA-TMB(0.75) silica material, spherical particles magnified

Fig. 9 and Fig. 10 show that for the samples labeled as SBA-TMB(0.15) and SBA-TMB(0.75) the formation of spherical particles is well-defined with an increase in the TMB: P123 mass ratio. This result evidences that adding more quantity of TMB leads to swell pore diameter in SBA-15 [11, 15, 56]. Fibrous particles turned into spherical particles.

In this approach it has been previously reported that there is 2D to 3D transition from SBA-15 to MCF particles with the increase in the TMB in the mixture synthesis [56]. In this case there are spherical particles with a wide particle size distribution, indicating that controlling the particle size is difficult. There is an optimal mass ratio and a maximum load of TMB to expand the pores [15, 16]. Spherical particles observed resemble MCF particles [56-58]. Moreover, it can be only stated that fibrous SBA-15 morphology was changed to spherical morphology by the addition of TMB.

3.1.4 Catalysts and supports proton affinity distributions (PAD)

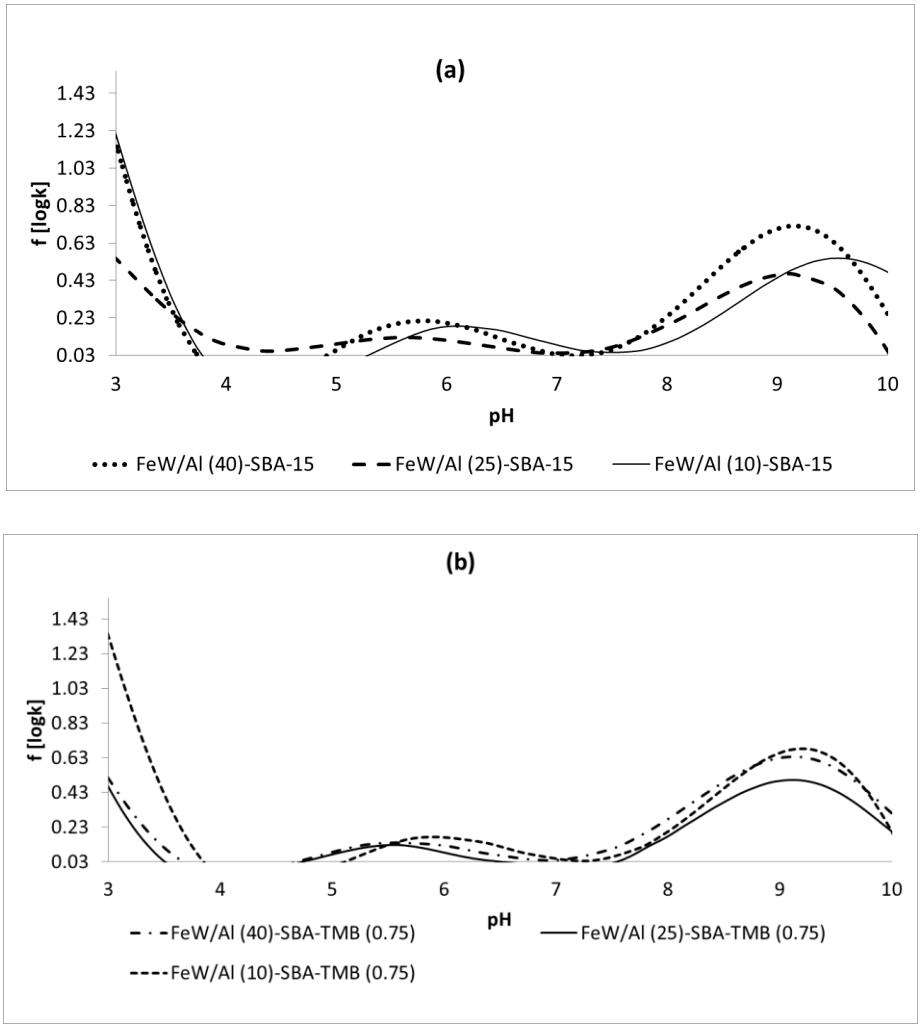

Fig. 11. PAD smoothed curves for non-activated catalysts, (a) Fe-W/Al(x)-SBA-15, (b) Fe-W/Al(x)-SBA-15-TMB(0.75), (x)= Si/Al molar ratio

Fig. 11 shows PAD curves for the catalysts prepared with the Al(x)-SBA-15 and Al(x)-SBA-TMB(0.75) materials. It is evidenced three principal peaks associated for type III (pH< 3.5) and IIA (3.5<pH< 5.5) acid sites, silanol (pH=6), siloxane (pH=9) and a mixed group (silanol and siloxane, pH>9) bonds for both kinds of catalysts. For the catalysts Fe-W/Al(40)-SBA-15 and Fe-W/Al(25)-SBA-15 a leftwards displacement was found, therefore, representing the formation of Brönsted acid sites

in the terminal silanol bonds of the catalyst. The same effect is evidenced for Fe-W/Al(x)-SBA-TMB(0.75) catalysts (Fig. 11 (b)).

Table 2 shows that Al(10)-SBA-15 support showed the highest overall acidity, due to the lower content of weak acidity bonds (silanol and siloxane) in comparison to the others Al(x)-SBA-15 supports. Therefore, indicating that higher Al content leads to the formation of acidity on the supports. Specifically Al(40)-SBA-15 support possesses more type III acid sites in comparison with the others SBA-15 supports.

Al(10)-SBA-TMB(0.75) is also the most acid (overall acidity) TMB modified support, despite of not evidencing the higher content of type III acid sites. It is also confirmed due to the decrease in the weak acid sites (silanol and siloxane bonds) content for this support. Meanwhile for the other TMB supports there is an increase in the content of silanol and the mixed group. This group is similar to IA group in terms of acidity [59].

Table 2. PAD quantification of acid sites.

Sample	Acid sites [mmol H^+g^{-1} cat]		
	III (*pH)	**Silanol (*pH)**	**Mixed Group (IA) (*pH)**
Al(10)-SBA-15	1.14 (3.104)	0.91 (5.56)	2.35(9.31)
Al(25)-SBA-15	0.66(3.185)	1.55(6.21)	0.9405(8.94)
Al(40)-SBA-15	2.27(3.061)	23.54(5.71)	5.472(8.45)
Al(10)-SBA-TMB(0.75)	0.506(3.098)	1.045(5.49)	1.649(8.525)
Al(25)-SBA-TMB(0.75)	1.366(3.21)	3.1603(5.32)	8.993(8.99)
Al(40)-SBA-TMB(0.75)	1.233(3.16)	11.137(5.36)	3.972(9.8)
Fe-W/Al(10)-SBA-15	1.577 (3.01)	3.210 (5.42)	5.290(9.31)
Fe-W/Al(25)-SBA-15	1.213(3.08)	5,632(5.61)	25.556(9.21)

Fe-W/Al(40)-SBA-15	1.816(3.061)	5.888(5.23)	10.294(9.96)
Fe-W/Al(10)-SBA-TMB(0.75)	2.573(3.13)	7.772(5.64)	20.540(9.26)
Fe-W/Al(25)-SBA-TMB(0.75)	0.536(3.064)	2.749(5.54)	3.214(9.45)
Fe-W/Al(40)-SBA-TMB(0.75)	0.669(3.21)	3.269(5.34)	4.124(9.86)

*Indicates the pH value where the peak was identified

The catalyst with greater acid strength (type III, based on the distribution of acid sites of the alumina) is the catalyst Fe-W/Al(40)-SBA-15. At lower Si/Al ratio (10) there is a greater amount of Al and by the limited textural properties of SBA-15 compared to SBA-TMB(0.75) there is a lower concentration of type III acid sites as it's reported in Table 2. This result indicates that higher Si/Al molar ratio contributed to generate more strong acid sites as expected [42, 60].

There is also reported a significant change in the overall acidity when metals are incorporated. It is shown in Fig. 11 (b), and Table 2 for Fe-W/Al(x)-SBA-15 and Fe-W/Al(x)SBA-TMB(0.75) catalysts. It was only evidenced an increase in the concentration of acid sites related to the mixed group, which indicates that the incorporation of active phases had a negative effect in the overall acid strength of the catalysts as reported in Table 2.

3.1.5 ^{27}Al MAS NMR solid measurements

Fig 12, 13 and 14 show the ^{27}Al MAS NMR spectrum for samples Al(x)-SBA-15 and Al(x)-SBA-TMB(0.75). These materials exhibit two clear signals at a chemical shift, ∂ = 0 ppm for AlO_6 octahedral coordination group, which is characteristic of the presence of extra structural aluminum species and other signal at ∂ = 52.9 ppm corresponding to AlO_4 tetrahedral aluminum species[61].

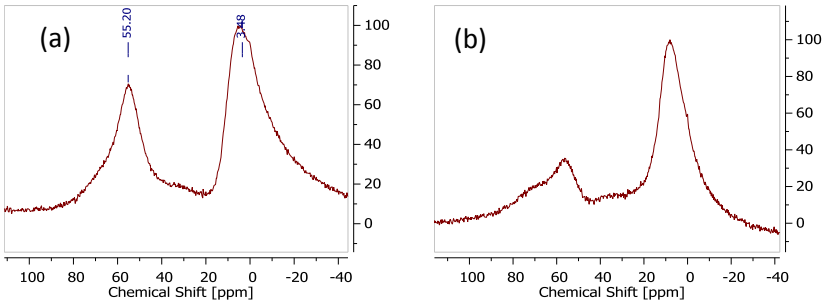

Fig. 12. ^{27}Al MAS NMR spectra Al modified supports, (a) Al(10)-SBA-15, (b) Al(10)-SBA-TMB(0.75)

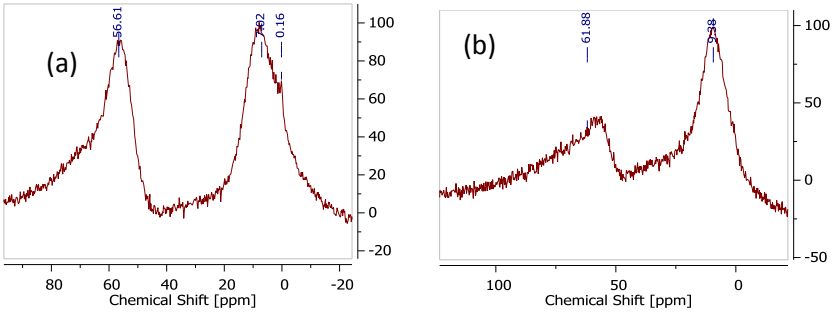

Fig. 13. ^{27}Al MAS NMR spectra Al modified supports, (a) Al(25)-SBA-15, (b) Al(25)-SBA-TMB(0.75)

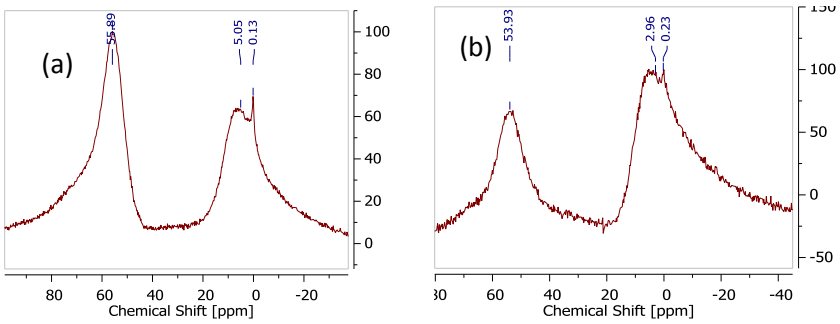

Fig. 14. ^{27}Al MAS NMR spectra Al modified supports, (a) Al(40)-SBA-15, (b) Al(40)-SBA-TMB(0.75)

In all cases, it was identified that for samples prepared with a Si/ Al molar ratio of 40 there was a greater incorporation of Al within the lattice of Si to form the material as illustrates Fig. 15 for tetrahedral aluminum coordination. This result confirms the formation of brönsted acid sites for catalysts for all catalysts, but in major proportion with the highest Si/Al molar ratio catalysts. Octahedral aluminum species are found in higher proportion on Al(x)-SBA-TMB(0.75) supports for the Si/Al molar ratio of 40

support, instead of Al(x)-SBA-15 supports as depicted Fig. 15 (b). It may be directly associated to the changes on morphology by adding TMB as a micellar swelling agent, then, varying the acid sites distribution therein.

The post synthesis method of incorporation or "chemical grafting" proposed to incorporate on the silica framework aluminum species was satisfactory to generate the acid strength distribution to the material on the surface of catalysts supported on these modified silica[62].

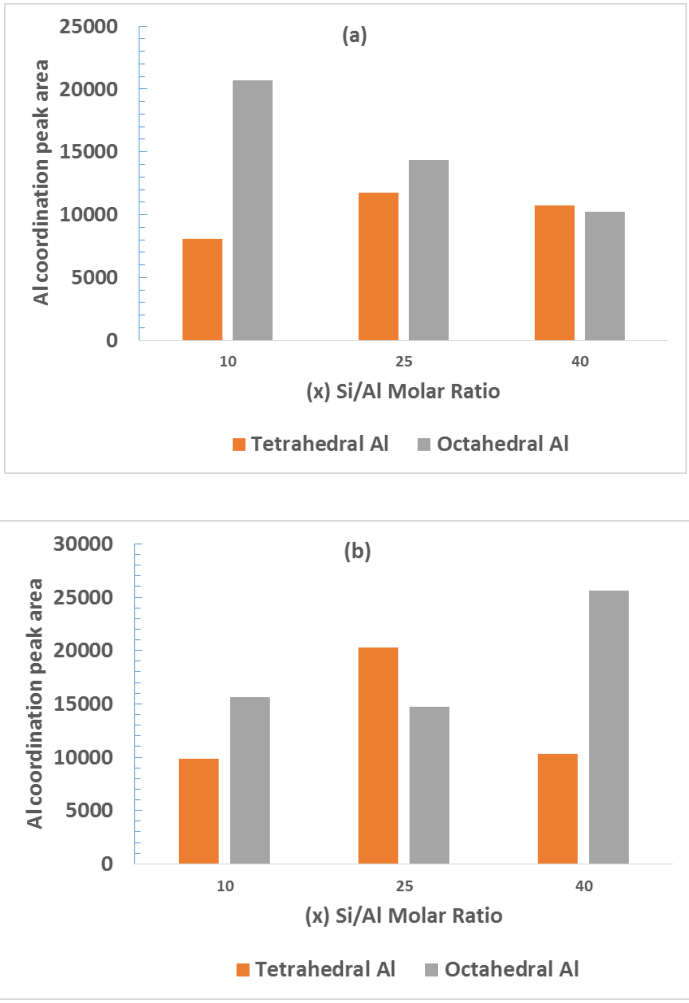

Fig. 15. Al species peak area for ^{27}Al MAS NMR, (a) Al(x)-SBA-15, (b) Al(x)-SBA-TMB(0.75), (x) indicates Si/Al molar ratio

These results are consistent with the PAD curves, which showed that the materials with higher density of type III acid sites were Al(40)-SBA-15 and Al(40)-SBA-TMB(0.75). It is known that the tetrahedral coordination is a precursor of Brönsted acid sites and octahedral for Lewis acid sites [7, 26-29, 63].

3.2 CATALYTIC EVALUATION

3.2.1 Preliminary paraffins hydrocracking tests

At the reaction conditions (350ºC, PH_2=2.2 MPa, and 4 h) neither n-hexadecane or 2,6,10,14-tetramethylpentadecane were converted by the sulfided catalyst Fe-W/Al(10)-SBA-TMB(0.75) despite of having the highest aluminum content. This no conversion effect can be explained on the basis that linear or multi-branched hydrocarbons required high hydrogenation capacity of the metallic active phases, this hydrogenation function enables the bi-functional mechanism required for hydrocracking as it has been previously reported for Pt/Al-SBA-15 catalysts[27].

3.2.2 Sulfided catalysts activity in the phenanthrene hydrocracking tests

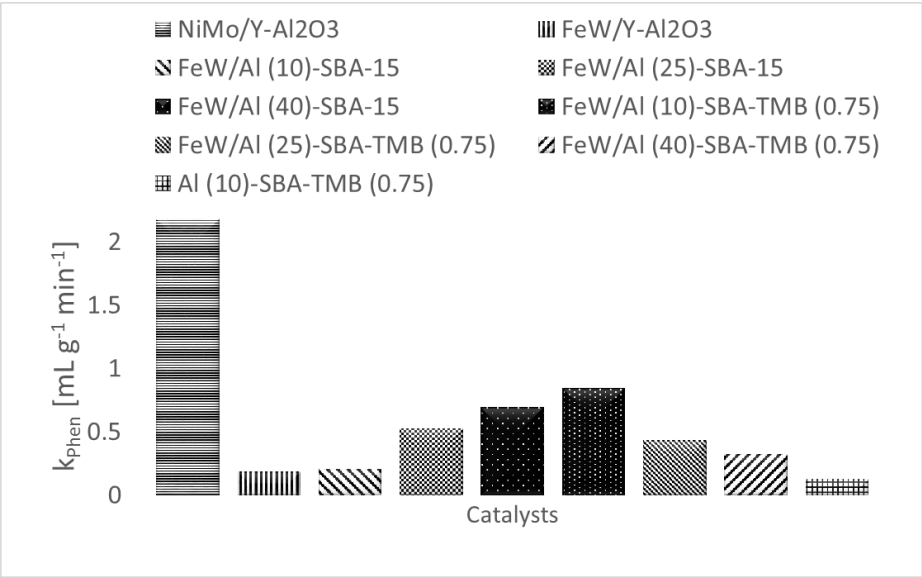

Fig. 16. Sulfided catalysts initial rate constants

Fig. 16 shows the activity of the catalysts evaluated. The catalyst which shows a higher initial rate constant is the conventional and commercial Ni-Mo/ɣ-Al_2O_3 catalyst (2.13 mL g^{-1} min^{-1}). The outstanding activity indicates an enhanced hydrogenation function of commercial catalyst in comparison with the catalyst prepared and presented in this study. However, among the SBA-15 based catalysts prepared, the catalyst Fe-W/Al(10)-SBA-TMB(0.75) resulted more active in comparison with the other Al-modified TMB catalysts and pristine Al(x)-SBA-15 supported catalysts.

3.2.3 Catalysts selectivity

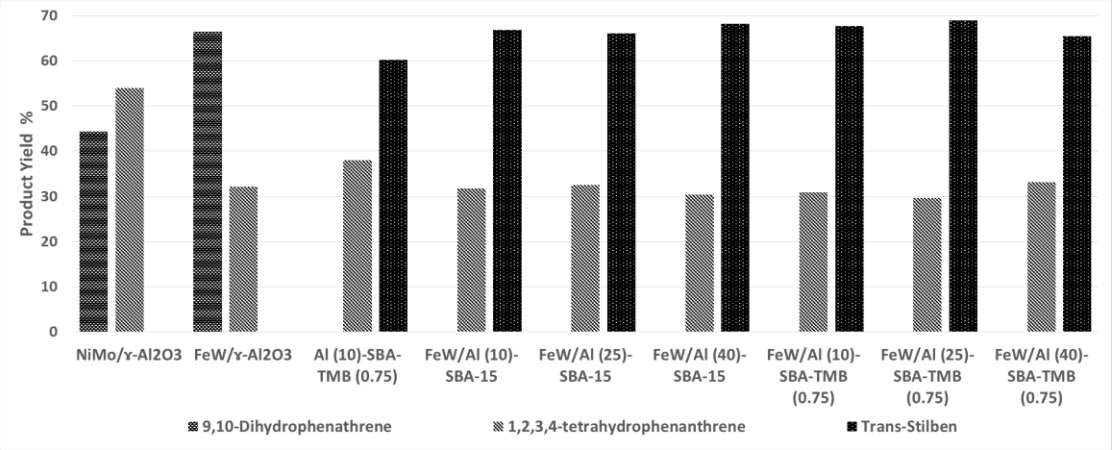

Fig. 17. Sulfided catalysts tested selectivity at 7.3 % of conversion

Fig. 17 depicts the iso-conversion selectivity towards the most abundant condensable products obtained at the reaction conditions. Selectivity is analyzed at that conversion (7.3 %) in order to observe the effect in the selectivity with Fe-W/ ɣ-Al_2O_3 catalyst and Al(10)-SBA-TMB(0.75) support, which shown the lowest initial rate constants.

The catalysts are selective to three majoritarian compounds (9,10-dihydrophenanthrene, 1,2,3,4-tetrahydrophenanthrene and trans-stilben). For commercial catalyst Ni-Mo/ɣ-Al_2O_3 and Fe-W/ɣ-Al_2O_3 selectivity tends to

hydrogenated compounds uniquely as shown Fig. 15. But, for Al(x)-SBA-15 and Al(x)-SBA-TMB supported catalysts, Fe-W/Al(40)-SBA-15 is slightly more selective to trans-stilben, which is a compound of aromatic ring opening. Al(x)-SBA-TMB(0.75) catalysts showed no significant differences in terms of selectivity at iso-conversion analysis.

4 DISCUSSION

This chapter discusses the individual effect of textural and acid properties for all Fe-W catalysts supported on Al(x)-SBA-15 and Al(x)-SBA-TMB(0.75). Fe-W catalysts were sulfided before the reaction as shown in chapter 3 (section 3.5), in addition the acidity measurements by ^{27}Al MAS NMR and PAD were conducted for Al modified supports and the oxidized Fe-W catalysts respectively (section 3.4.4). The changes in acidity of the sulfided catalysts compared to oxidized precursors of the catalysts can be correlated, since the changes in acidity from sulfided species to oxidized species vary in the same proportion as it has been previously stated in the literature for hydro processing experiments with SBA-15 type supports[8-10]. Moreover, the formation of acid sites and their influence on the hydrocracking reaction is attributed to Al incorporation on the surface of the catalytic supports as depicted ^{27} Al MAS NMR analyses, which was not changed by the process of sulfidation of the oxide catalysts precursors, which acidity was measured by PAD (section 4.1.4).

4.1 EFFECT OF THE ACID PROPERTIES IN THE HCK OF PHENANTHRENE

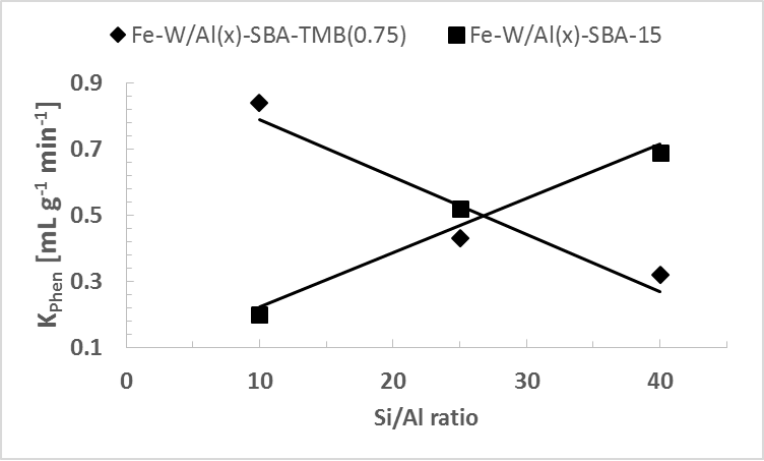

Fig. 18. Effect of Si/Al ratio in the sulfided catalysts activity

The effect of Si/Al molar ratio on the performance of catalysts is clarified in Fig. 18. For Al(x)-SBA-15 supported catalysts series the most active was the catalyst with

Si/Al molar ratio of 40. This result is directly correlated to ^{27}Al MAS NMR results, which evidenced higher tetrahedral Al ions incorporated to this catalyst in major proportion than for the other catalysts with different Si/Al molar ratios prepared, this is shown in Fig. 15 (section 4.1.5).

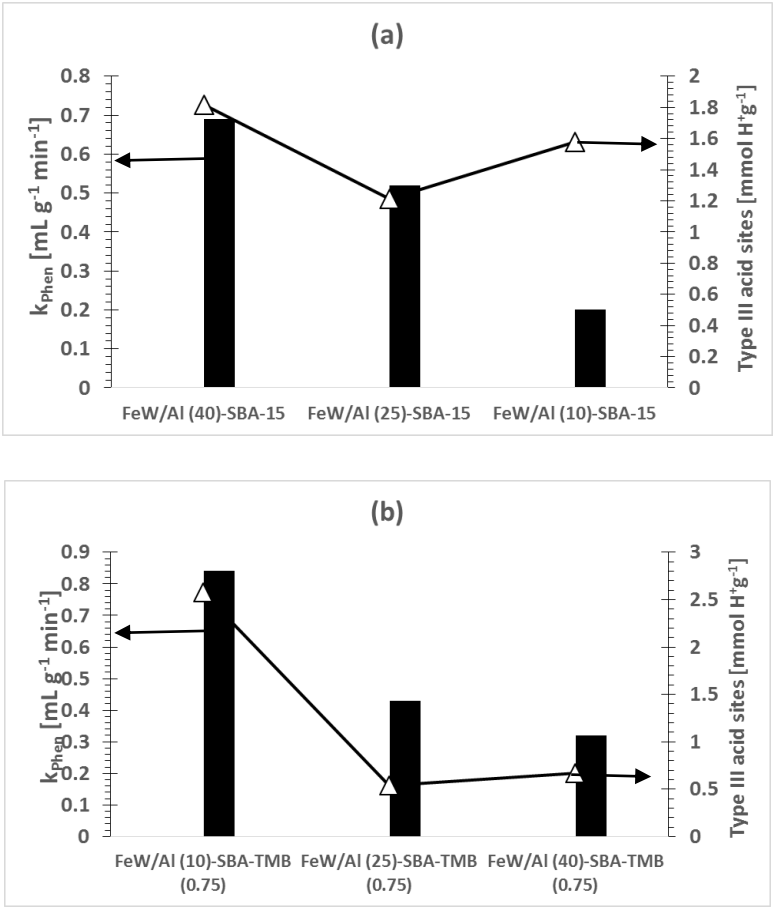

Fig. 19. Sulfided catalysts activity and Type III acid sites correlation, (a) Fe-W/Al(x)-SBA-15, (b) Fe-W/Al(x)-SBA-TMB(0.75), (x)= Si/Al molar ratio

Fig. 19 illustrates the effect of the strong acid sites contents (type III sites quantified by Gaussian deconvolution of the measured PAD in section 4.1.4) on the catalysts activity, it also confirmed that the catalysts with higher content of type III acid sites (based on alumina acid sites distribution) are the catalysts which showed enhanced activity, therefore, the strong acidity attributed to type III acid sites influenced the rate of formation of products. For Al(x)-SBA-15 supported catalysts, it is noteworthy that

at the highest Al content (Si/Al=10) there is not direct correlation with activity and type III acid sites content as depicted Fig 19.(a), suggesting that the activity improvement is less promoted by strong acidity on the surface of the catalyst with those supports. For catalysts supported on Al(x)-SBA-TMB(0.75), the catalyst with Si/Al molar ratio of 10 is the most active and also possesses the highest amount of type III acid sites as shown in Fig. 19 (b). Sulfided catalysts activity and type III acid sites content is perfectly correlated with this kind of catalysts, thus, the formation of stronger acid sites on the hydrocracking reaction enhanced the catalytic activity for TMB modified catalysts.

The order of activity by changing the Si/Al molar ratios is: Fe-W/Al(40)-SBA-15 > Fe-W/Al(25)-SBA-15>Fe-W/Al(10)-SBA-15, in contrast to the Fe-W/ Al(x)-SBA-TMB(0.75) sulfided catalysts, the order of activity is the opposite: Fe-W/Al(10)-SBA-TMB(0.75)>Fe-W/Al(25)-SBA-TMB(0.75)>Fe-W/Al(40)-SBA-TMB(0.75). This effect can be attributed to the less ordering on the surface of those catalysts, therefore, the formation of extra-structural aluminum species is predominant, decreasing the activity, as it has been previously reported [26].

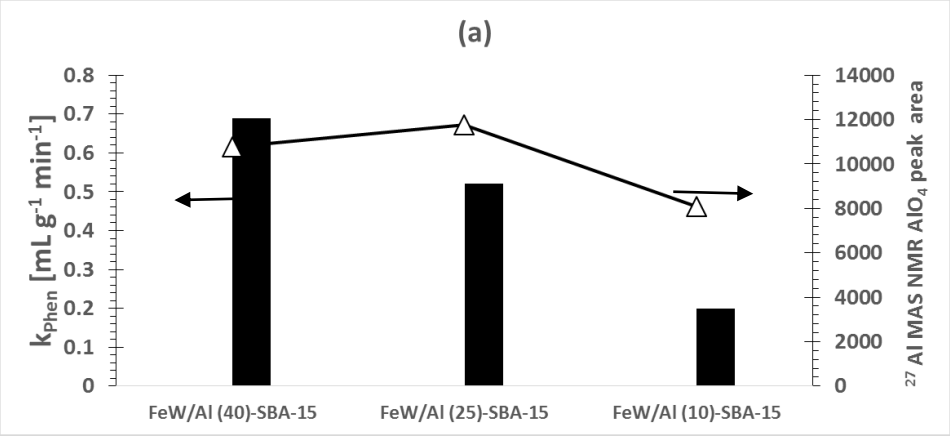

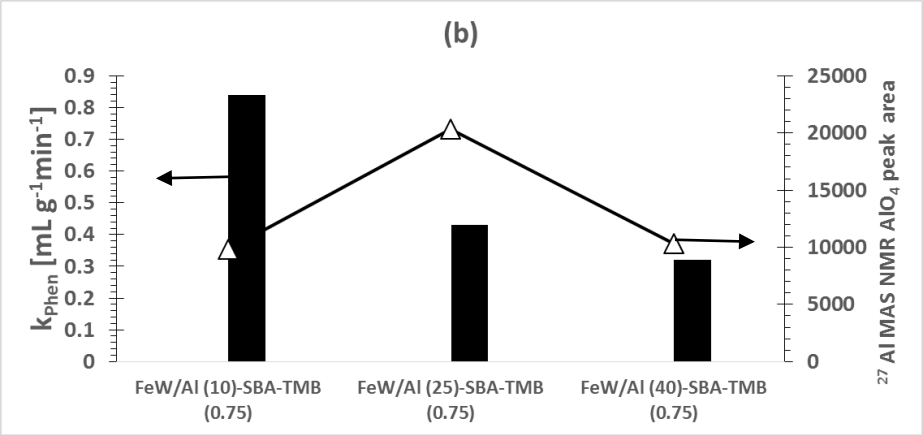

Fig. 20. Sulfided catalysts activity correlated to AlO_4 species, (a) Fe-W/Al(x)-SBA-15, (b) Fe-W/Al(x)-SBA-TMB(0.75), (x)= Si/Al molar ratio

The effect on catalysts activity by the formation of tetrahedral aluminum acid sites is shown in Fig. 20, it can be inferred that there is a correlation between the AlO_4 peak areas with the activity of the sulfided catalysts. In that sense, tetrahedral aluminum incorporation generates the Brönsted acid sites contribution to the overall acidity of the catalysts and supports, and it also influenced isomerization and cracking reactions as expected [19-22, 34, 61, 64]. This effect is more apparent for the catalysts supported on Al(x)-SBA-15 for the Si/Al molar ratio of 40, instead of the series of catalysts supported on Al(x)-SBA-TMB(0.75), indicating that the change on the surface morphology of the silica supports as evidenced by SEM micrographs (section 4.1.3) influenced the distribution of acid sites on the surface of the catalysts prepared by using Al(x)-SBA-TMB(0.75) supports. It was also marked by the ^{27}Al MAS NMR spectra for Al(x)-SBA-15 supports, which exhibited a better formation of the peaks associated to Brönsted acid sites (section 4.1.5).

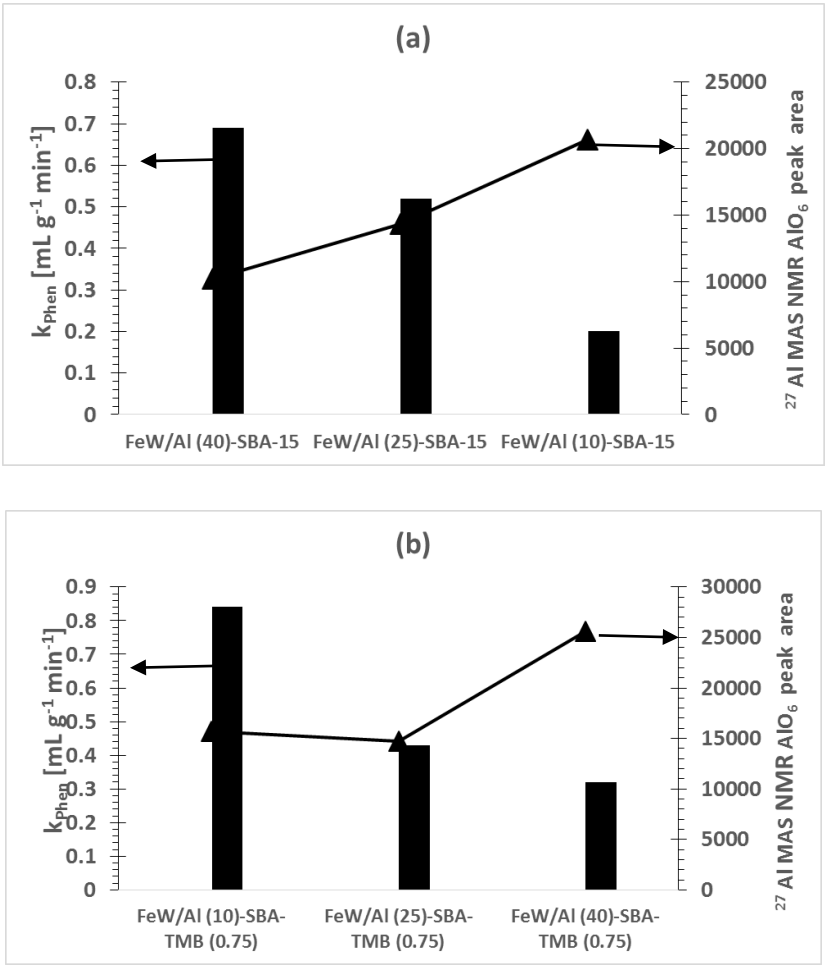

Fig. 21. Sulfided catalysts activity correlated to AlO_6 species, (a) Fe-W/Al(x)-SBA-15, (b) Fe-W/Al(x)-SBA-TMB(0.75), (x)= Si/Al molar ratio

According to Fig. 21, there is not direct influence of octahedral aluminum incorporation in the activity of both series of sulfided catalysts, neither Fe-W/Al(x)-SBA-15 or Fe-W/Al(x)-SBA-TMB(0.75). This result proposes that catalysts activity is less promoted for Lewis acidity attributed to extra-framework aluminum species.

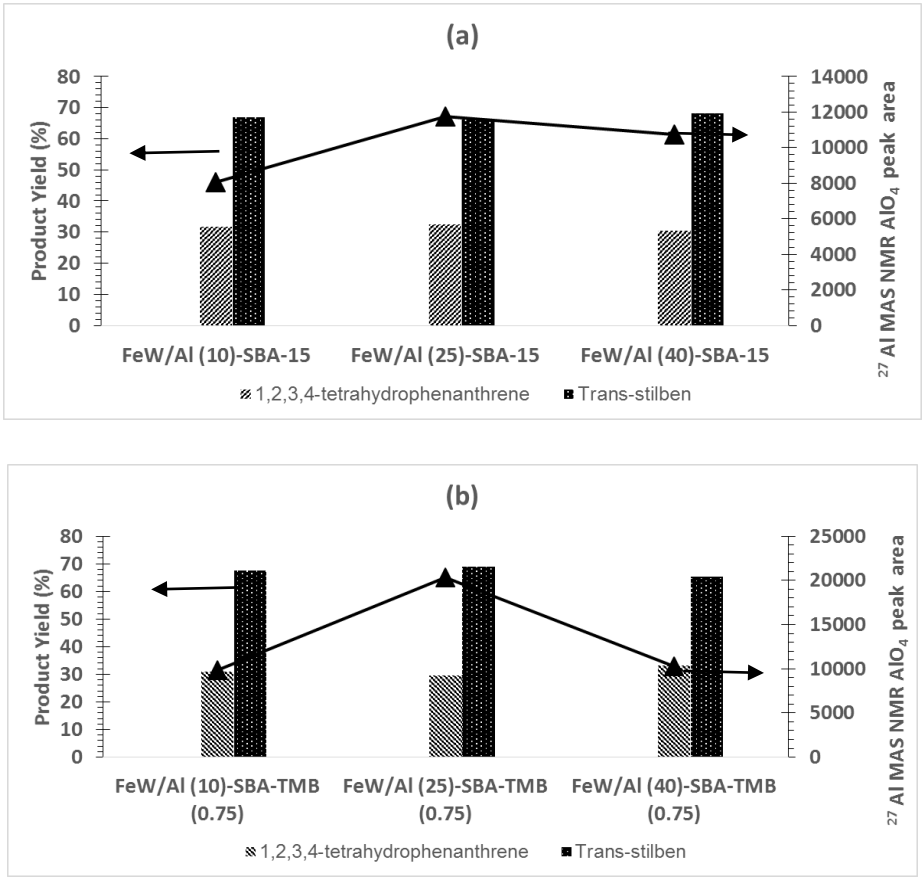

Fig. 22. Sulfided catalysts selectivity correlated to AlO_4 species, (a) Fe-W/Al(x)-SBA-15, (b) Fe-W/Al(x)-SBA-TMB(0.75), (x)= Si/Al molar ratio

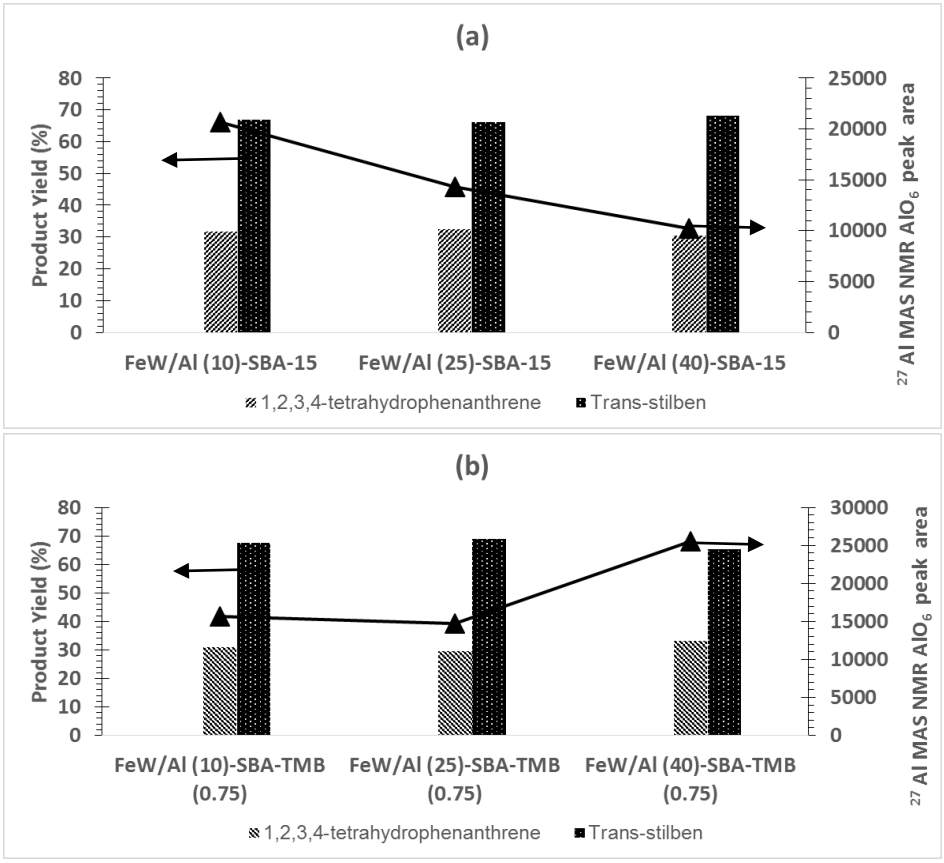

Fig. 22. Sulfided catalysts selectivity correlated to AlO_6 species, (a) Fe-W/Al(x)-SBA-15, (b) Fe-W/Al(x)-SBA-TMB(0.75), (x)= Si/Al molar ratio

In terms of the selectivity the formation of rupture compounds such as trans-stilben can be attributed to the effect of Al incorporation because Al(x)-SBA-15 catalysts are more selective to this compound in Si/Al molar ratios when tetrahedral Al incorporation is found in higher proportion as shown in Fig. 21. Tetrahedral aluminum incorporation had a direct correlation with the formation of trans-stilben, which evidenced a slight enhancement in selectivity for the catalysts prepared with the Si/Al molar ratio of 25.

In comparison to octahedral aluminum incorporation as shown in Fig. 22, no effect on sulfided catalysts selectivity can be observed, therefore, it's confirmed the effect of tetrahedral Al incorporation in the selectivity of phenanthrene hydrocracking reaction. Tetrahedral aluminum species are precursors of Brönsted acid sites, which

in terms of acidity are stronger than Lewis acid sites related to octahedral aluminum species, this was also evidenced by Dai *et al*., who tested Ni-W/Al-SBA-15 catalysts in the hydrocracking of a VGO, demonstrating that Al-SBA-15 catalysts induced high selectivity to MD as a result of a higher tetrahedral aluminum incorporation [26].

4.2 EFFECT OF THE TEXTURAL PROPERTIES IN THE HCK OF PHENANTHRENE

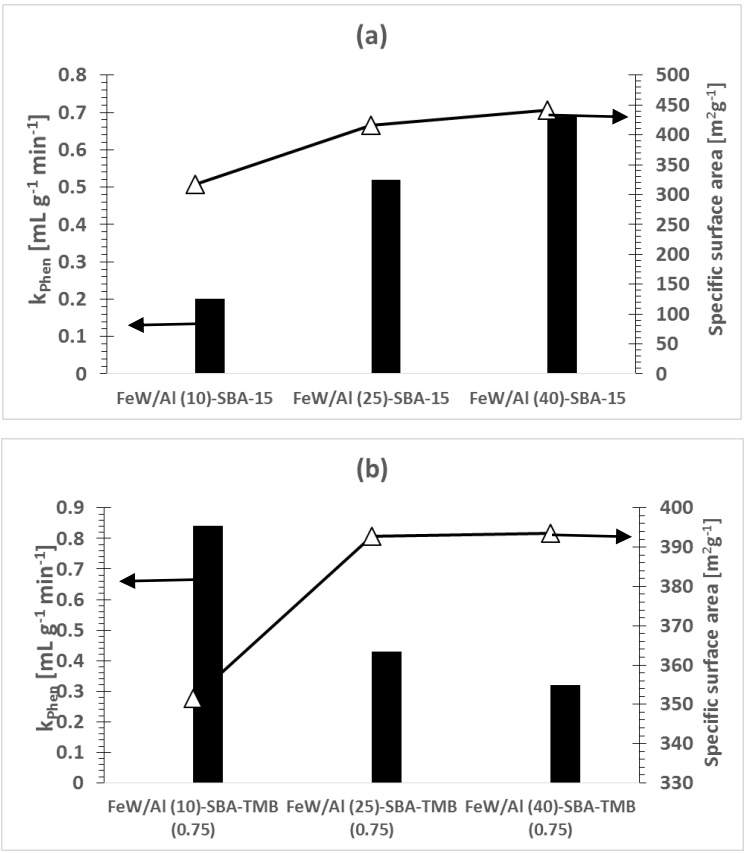

Fig. 23. Sulfided catalysts activity correlated to S_{BET}, (a) Fe-W/Al(x)-SBA-15, (b) Fe-W/Al(x)-SBA-TMB(0.75), (x)= Si/Al molar ratio

Fig. 23 (a) displays the catalytic activity of all SBA-15 based catalysts correlated with the specific surface area (S_{BET}), establishing the effect of specific surface area in the catalytic activity. Fe-W/Al(40)-SBA-15 is the catalyst which showed the higher activity with the highest S_{BET} (m^2g^{-1}); Fe-W/Al(40)-SBA-15 is also the catalyst with higher pore size and pore volume as shown in Table 1 (section 4.1), demonstrating

that catalysts with larger pore volume and pore diameter lead to products easily than lower pore sizes and pore volumes catalysts.

On the contrary for Al(x)-SBA-TMB(0.75) supported catalysts, the sulfided catalyst with the lowest catalytic activity is Fe-W/Al(40)-SBA-TMB(0.75) despite of having the highest surface area in comparison to Fe-W/Al(10)-SBA-TMB(0.75) as shown in Fig. 23 (b). Therefore, there is not a direct correlation of S_{BET} with the catalytic activity of this type of catalysts.

To provide a better explanation to this behavior wide angle XRD patterns (Fig. 5 section 4.1.2) made it possible to establish that catalysts with higher specific surface area, but higher pore volumes have enabled the formation of metallic phase's agglomerations, it is due to the decrease in the mesostructured ordering pattern of SBA-15 by the addition of TMB to expand its pores in Al(x)-SBA-TMB(0.75) supported catalysts as shown in Fig. 4 (section 4.1.2). Therefore, the catalytic activity with TMB modified catalysts was diminished despite of their larger pore sizes. In addition, the previous highlighted results ratify that catalytic activity was also influenced by the interactions that sulfided metallic phases had with the acid sites on the surface of the supports, as it was stated in the previous section (5.1), since acidity measurements correlations with sulfided catalysts fitted better for Al(x)-SBA-15 catalysts rather than Al(x)-SBA-TMB(0.75) catalysts, hence, the method of preparation of catalysts may have promoted the formation of clusters of metallic phases as observed, and consequently a better dispersion of metallic phases and acid sites may be found for Al(x)-SBA-15 rather than Al(x)-SBA-TMB(0.75) sulfided catalysts, providing a plausible explanation of their activity.

4.3 EFFECT OF THE Fe-W ACTIVE PHASES IN THE HCK OF PHENANTHRENE

To evaluate the effect of Fe-W sulfided active phases in the hydrocracking of phenanthrene, a reaction was performed with the Al modified support, Al(10)-SBA-TMB(0.75); as shown in Fig. 16 (section 4.2.2) the catalytic activity with this support is limited to 0.12 [mL g^{-1} min^{-1}] in comparison to 0.84 [mL g^{-1} min^{-1}] after sulfided Fe-

W active phases are incorporated for the same support. Therefore, it has been proved that sulfided metallic phases are required to direct the reaction towards the desired products, and to increase the catalyst activity and product yield. Moreover HCK reactions require bifunctional catalysts to enhance product yield and conversion, which has been indicated for several authors [23-26]. In this case, Fe-W sulfided active phases exhibited a different product distribution compared to Ni-Mo sulfided active phases on the commercial catalyst. This product distribution yielded to more selective rupture compounds in the hydrocracking of phenanthrene (trans-stilben) for sulfided Fe-W catalysts supported on post synthesis Al incorporated silica. It's noteworthy that Fe-W/γ-Al_2O_3 sulfided catalyst did not show the same product distribution, confirming that Al-modified silica supports enhance the production of rupture compounds associated with the acid site distribution therein, instead of sulfided Fe-W active phases.

5 CONCLUSIONS

- The synthesis parameters in SBA-15 mesostructured silica preparation were modified, this modification leaded to get larger pore diameter mesoporous silica by adding micellar expansion agents such as TMB. This swelling effect of TMB expanded pores to change morphology from a hexagonal array of tubular channels into spherical nanoparticles.
- Adding small amounts of NH_4F before TEOS incorporation during the synthesis for SBA-15 silica yielded in amorphous silica with higher pore diameters, but there was a significant loss in the specific surface area. Therefore, NH_4F additions disfavored ordering before TEOS incorporation at the initial reaction temperature.
- Post-synthesis Al-SBA-15 based silicate was successfully tested as support for Fe-W sulfided catalysts in phenanthrene hydrocracking reaction, with this incorporation all sulfided catalysts were selective to rupture compounds related to the presence of brönsted acidity; this effect is also attributed to tetrahedral aluminum species formed, and confirmed by ^{27}Al MAS NMR analyses.
- Sulfided Fe-W active phases in hydrocracking of phenanthrene has been tested and showed a lower hydrogenation activity than Ni-Mo sulfided active phases, but supported on Al-modified silica enhanced activity towards ring opening compounds, therefore, it opened a new insight in the reactivity and selectivity of less expensive active phases in hydro conversion processes.

REFERENCES

[1] J.L. Agudelo, B. Mezari, E.J.M. Hensen, S.A. Giraldo, L.J. Hoyos, On the effect of EDTA treatment on the acidic properties of USY zeolite and its performance in vacuum gas oil hydrocracking, Applied Catalysis A: General, 488 (2014) 219-230.

[2] S. Ahmed Ali, M. Elias Biswas, T. Yoneda, T. Miura, H. Hamid, E. Iwamatsu, H. Al-Suaibi, A novel catalyst for heavy oil hydrocracking, in: H. Hideshi, O. Kiyoshi (Eds.) Studies in Surface Science and Catalysis, Elsevier, 1999, pp. 407-410.

[3] A.M. Alsobaai, R. Zakaria, B.H. Hameed, Hydrocracking of petroleum gas oil over NiW/MCM-48-USY composite catalyst, Fuel Processing Technology, 88 (2007) 921-928.

[4] H. Ortiz-Moreno, J. Ramírez, F. Sanchez-Minero, R. Cuevas, J. Ancheyta, Hydrocracking of Maya crude oil in a slurry-phase batch reactor. II. Effect of catalyst load, Fuel, 130 (2014) 263-272.

[5] J.P. Franck, J.F. Le page, Catalysts for the Hydrocracking of Heavy Gas Oils into Middle Distillates, in: T. Seiyama, K. Tanabe (Eds.) Studies in Surface Science and Catalysis, Elsevier, 1981, pp. 792-803.

[6] C.R. Lahiri, D. Biswas, High pressure hydrocracking of vacuum gas oil to middle distillates, Physica B+C, 139–140 (1986) 725-728.

[7] X. Sun, H. Fan, J. Zhu, Effect of addition of Y-Al-SBA-15 composite zeolite on catalyst performance in hydrocracking, Shiyou Huagong/Petrochemical Technology, 42 (2013) 518-523.

[8] P.E. Boahene, K.K. Soni, A.K. Dalai, J. Adjaye, Application of different pore diameter SBA-15 supports for heavy gas oil hydrotreatment using FeW catalyst, Applied Catalysis A: General, 402 (2011) 31-40.

[9] P.E. Boahene, K.K. Soni, A.K. Dalai, J. Adjaye, Hydroprocessing of heavy gas oils using FeW/SBA-15 catalysts: Experimentals, optimization of metals loading, and kinetics study, Catalysis Today, (2012).

[10] K. Chandra Mouli, K. Soni, A. Dalai, J. Adjaye, Effect of pore diameter of Ni–Mo/Al-SBA-15 catalysts on the hydrotreating of heavy gas oil, Applied Catalysis A: General, 404 (2011) 21-29.
[11] R.N. Widyaningrum, T.L. Church, M. Zhao, A.T. Harris, Mesocellular-foam-silica-supported Ni catalyst: Effect of pore size on H_2 production from cellulose pyrolysis, International Journal of Hydrogen Energy, 37 (2012) 9590-9601.
[12] E. Byambajav, Hydrocracking of asphaltene with metal catalysts supported on SBA-15, Applied Catalysis A: General, 252 (2003) 193-204.
[13] B. Li, J. Xu, X. Li, J. Liu, S. Zuo, Z. Pan, Z. Wu, Bimetallic iron and cobalt incorporated MFI/MCM-41 composite and its catalytic properties, Materials Research Bulletin, 47 (2012) 1142-1148.
[14] X. Zhang, F. Zhang, X. Yan, Z. Zhang, F. Sun, Z. Wang, D. Zhao, Hydrocracking of heavy oil using zeolites Y/Al-SBA-15 composites as catalyst supports, Journal of Porous Materials, 15 (2007) 145-150.
[15] D. Zhao, J. Feng, Q. Huo, N. Melosh, G.H. Fredrickson, B.F. Chmelka, G.D. Stucky, Triblock Copolymer Syntheses of Mesoporous Silica with Periodic 50 to 300 Angstrom Pores, Science, 279 (1998) 548-552.
[16] D. Zhao, Y. Wan, Chapter 8 The synthesis of mesoporous molecular sieves, in: H.v.B.A.C. Jiří Čejka, S. Ferdi (Eds.) Studies in Surface Science and Catalysis, Elsevier, 2007, pp. 241-III.
[17] M. Song, C. Zou, G. Niu, D. Zhao, Improving the Hydrothermal Stability of Mesoporous Silica SBA-15 by Pre-treatment with $(NH_4)_2SiF_6$, Chinese Journal of Catalysis, 33 (2012) 140-151.
[18] K. Waldron, Z. Wu, D. Zhao, X.D. Chen, C. Selomulya, On the improvement of pore accessibility through post-synthesis hydrothermal treatments of spray dried SBA-15 microspheres, Chemical Engineering Science, 127 (2015) 276-284.
[19] S. Garg, K. Soni, G.M. Kumaran, M. Kumar, J.K. Gupta, L.D. Sharma, G.M. Dhar, Effect of Zr-SBA-15 support on catalytic functionalities of Mo, CoMo, NiMo hydrotreating catalysts, Catalysis Today, 130 (2008) 302-308.

[20] M. Gómez-Cazalilla, A. Infantes-Molina, R. Moreno-Tost, P.J. Maireles-Torres, J. Mérida-Robles, E. Rodríguez-Castellón, A. Jiménez-López, Al-SBA-15 as a support of catalysts based on chromium sulfide for sulfur removal, Catalysis Today, 143 (2009) 137-144.
[21] G. Muthu Kumaran, S. Garg, K. Soni, M. Kumar, L.D. Sharma, G. Murali Dhar, K.S. Rama Rao, Effect of Al-SBA-15 support on catalytic functionalities of hydrotreating catalysts: I. Effect of variation of Si/Al ratio on catalytic functionalities, Applied Catalysis A: General, 305 (2006) 123-129.
[22] T. Klimova, J. Reyes, O. Gutiérrez, L. Lizama, Novel bifunctional NiMo/Al-SBA-15 catalysts for deep hydrodesulfurization: Effect of support Si/Al ratio, Applied Catalysis A: General, 335 (2008) 159-171.
[23] Z. Lei, L. Gao, H. Shui, W. Chen, Z. Wang, S. Ren, Hydrotreatment of heavy oil from a direct coal liquefaction process on sulfided Ni–W/SBA-15 catalysts, Fuel Processing Technology, 92 (2011) 2055-2060.
[24] C. Liang, M.-C. Wei, H.-H. Tseng, E.-C. Shu, Synthesis and characterization of the acidic properties and pore texture of Al-SBA-15 supports for the canola oil transesterification, Chemical Engineering Journal, 223 (2013) 785-794.
[25] J.A. Mendoza-Nieto, I. Puente-Lee, C. Salcedo-Luna, T. Klimova, Effect of titania grafting on behavior of NiMo hydrodesulfurization catalysts supported on different types of silica, Fuel, 100 (2012) 100-109.
[26] Y. Dai, Y.S. Zhou, Q. Wei, Q.Y. Cui, Z. Qin, Influences of Al modification on the properties and catalytic performance of SBA-15 molecular sieves in hydrocracking, Ranliao Huaxue Xuebao/Journal of Fuel Chemistry and Technology, 41 (2013) 1502-1506.
[27] M.G. Seo, D.W. Lee, K.Y. Lee, D.J. Moon, Pt/Al-SBA-15 catalysts for hydrocracking of C_{21}-C_{34} n-paraffin mixture into gasoline and diesel fractions, Fuel, 143 (2015) 63-71.
[28] S. Zeng, J. Blanchard, M. Breysse, Y. Shi, X. Shu, H. Nie, D. Li, Post-synthesis alumination of SBA-15 in aqueous solution: A versatile tool for the preparation of

acidic Al-SBA-15 supports, Microporous and Mesoporous Materials, 85 (2005) 297-304.
[29] J. Zhu, J. Wang, X. Sun, J. Yang, Effect of Al-SBA-15 preparation method on the performance of hydrocracking catalyst with Al-SBA-15/USY composite support, Petroleum Processing and Petrochemicals, 43 (2012) 28-32.
[30] Y. Villasana, F. Ruscio-Vanalesti, C. Pfaff, F.J. Méndez, M.Á. Luis-Luis, J.L. Brito, Atomic ratio effect on catalytic performance of FeW-based carbides and nitrides on thiophene hydrodesulfurization, Fuel, 110 (2013) 259-267.
[31] G. Bellussi, G. Rispoli, A. Landoni, R. Millini, D. Molinari, E. Montanari, D. Moscotti, P. Pollesel, Hydroconversion of heavy residues in slurry reactors: Developments and perspectives, Journal of Catalysis, (2013).
[32] E. Benazzi, L. Leite, N. Marchal-George, H. Toulhoat, P. Raybaud, New insights into parameters controlling the selectivity in hydrocracking reactions, Journal of Catalysis, 217 (2003) 376-387.
[33] J. Francis, E. Guillon, N. Bats, C. Pichon, A. Corma, L.J. Simon, Design of improved hydrocracking catalysts by increasing the proximity between acid and metallic sites, Applied Catalysis A: General, 409-410 (2011) 140-147.
[34] T. Klimova, M. Calderón, J. Ramírez, Ni and Mo interaction with Al-containing MCM-41 support and its effect on the catalytic behavior in DBT hydrodesulfurization, Applied Catalysis A: General, 240 (2003) 29-40.
[35] J.T. Kloprogge, W.J.J. Welters, E. Booy, V.H.J. de Beer, R.A. van Santen, J.W. Geus, J.B.H. Jansen, Catalytic activity of nickel sulfide catalysts supported on Al-pillared montmorillonite for thiophene hydrodesulfurization, Applied Catalysis A: General, 97 (1993) 77-85.
[36] G.D. Stucky, B.F. Chmelka, D. Zhao, N. Melosh, Q. Huo, J. Feng, P. Yang, D. Pine, D. Margolese, W. Lukens, Block copolymer processing for mesostructured inorganic oxide materials, in, Google Patents, 2003.
[37] R.S.D.M. Montanari, IT), Marchionna, Mario (Milan, IT), Panariti, Nicoletta (Lecco, IT), Delbianco, Alberto (Magenta, IT), Rosi, Sergio (San Donato Milanese, IT) Process for the conversion of heavy feedstocks such as heavy crude oils and

distillation residues, in: US Patent 8,017,000, ENI S.p.A. (Rome, IT),SNAMPROGETTI S.p.A. (San Donato Milanese, IT),ENITECNOLOGIE S.p.A. (San Donato Milanese, IT), United States, 2011.
[38] Y.K. Park, H.W. Lee, J.K. Jeon, J. Han, C.U. Kim, S.Y. Jeong, K.E. Jeong, Hydroconversion of n-dodecane over nanoporous catalysts, Journal of Nanoscience and Nanotechnology, 13 (2013) 714-717.
[39] M. Lualdi, G. Di Carlo, S. Lögdberg, S. Järås, M. Boutonnet, V. La Parola, L.F. Liotta, G.M. Ingo, A.M. Venezia, Effect of Ti and Al addition via direct synthesis to SBA-15 as support for cobalt based Fischer-Tropsch catalysts, Applied Catalysis A: General, 443–444 (2012) 76-86.
[40] Y.H. Yue, A. Gédéon, J.L. Bonardet, J.B. d'Espinose, N. Melosh, J. Fraissard, Direct incorporation of Al in SBA mesoporous materials: characterization, stability and catalytic activity, in: S. Abdelhamid, J. Mietek (Eds.) Studies in Surface Science and Catalysis, Elsevier, 2000, pp. 209-218.
[41] J. Blanchard, M. Breysse, K. Fajerwerg, C. Louis, C.E. Hédoire, A. Sampieri, S. Zeng, G. Pérot, H. Nie, D. Li, Acidic zeolites and Al-SBA-15 as supports for sulfide phases: application to hydrotreating reactions, in: N.Ž. J. Čejka, P. Nachtigall (Eds.) Studies in Surface Science and Catalysis, Elsevier, 2005, pp. 1517-1524.
[42] W. Hu, Q. Luo, Y. Su, L. Chen, Y. Yue, C. Ye, F. Deng, Acid sites in mesoporous Al-SBA-15 material as revealed by solid-state NMR spectroscopy, Microporous and Mesoporous Materials, 92 (2006) 22-30.
[43] Y. Li, D. Pan, C. Yu, Y. Fan, X. Bao, Synthesis and hydrodesulfurization properties of NiW catalyst supported on high-aluminum-content, highly ordered, and hydrothermally stable Al-SBA-15, Journal of Catalysis, 286 (2012) 124-136.
[44] E. Byambajav, Y. Ohtsuka, Cracking behavior of asphaltene in the presence of iron catalysts supported on mesoporous molecular sieve with different pore diameters, Fuel, 82 (2003) 1571-1577.
[45] A.J.J. Koekkoek, J.A.R. van Veen, P.B. Gerrtisen, P. Giltay, P.C.M.M. Magusin, E.J.M. Hensen, Brønsted acidity of Al/SBA-15, Microporous and Mesoporous Materials, 151 (2012) 34-43.

[46] K. Jaroszewska, A. Masalska, K. Bączkowska, J.R. Grzechowiak, Conversion of decalin and 1-methylnaphthalene over AlSBA-15 supported Pt catalysts, Catalysis Today, 196 (2012) 110-118.
[47] K. Jaroszewska, A. Masalska, D. Marek, J.R. Grzechowiak, A. Zemska, Effect of support composition on the activity of Pt and PtMo catalysts in the conversion of n-hexadecane, Catalysis Today, 223 (2014) 76-86.
[48] F. Rouquerol, J. Rouquerol, K. Sing Adosrption by Powders and Porous Solids. Principles, Methodology and Applications.
[49] C. Contescu, J. Jagiello, J.A. Schwarz, Proton affinity distributions: A scientific basis for the design and construction of supported metal catalysts, in: J.M.B.D.P.A.J. G. Poncelet, P. Grange (Eds.) Studies in Surface Science and Catalysis, Elsevier, 1995, pp. 237-252.
[50] C. Contescu, V.T. Popa, J.B. Miller, E.I. Ko, J.A. Schwarz, Proton Affinity Distributions of TiO_2-SiO_2 and ZrO_2-SiO_2 Mixed Oxides and Their Relationship to Catalyst Activities for 1-Butene Isomerization, Journal of Catalysis, 157 (1995) 244-258.
[51] H. Knözinger, P. Ratnasamy, Catalytic Aluminas: Surface Models and Characterization of Surface Sites, Catalysis Reviews, 17 (1978) 31-70.
[52] B.S. Gevert, J.-E. Otterstedt, Upgrading of directly liquefied biomass to transportation fuels: catalytic cracking, Biomass, 14 (1987) 173-183.
[53] J. Rouquerol, D. Avnir, C.W. Fairbridge, D.H. Everett, J.H. Haynes, N. Pernicone, J.D. Framsay, K. Sing , K.K. Unger, Recommendations for the characterizations of porous solids (Technical Report), Pure & Appl. Chem, 66 (1994) 1739-1758.
[54] W.-H. Zhang, L. Zhang, J. Xiu, Z. Shen, Y. Li, P. Ying, C. Li, Pore size design of ordered mesoporous silicas by controlling micellar properties of triblock copolymer $EO_{20}PO_{70}EO_{20}$, Microporous and Mesoporous Materials, 89 (2006) 179-185.
[55] B. Dragoi, E. Dumitriu, S. Bennici, A. Auroux, Acidic and adsorptive properties of Al modified SBA-15 samples, in: P.M. Antoine Gédéon, B. Florence (Eds.) Studies in Surface Science and Catalysis, Elsevier, 2008, pp. 953-956.

[56] R. Fazaeli, H. Aliyan, M.A. Ahmadi, S. Hashemian, Host (aluminum incorporated mesocellulous silica foam (Al-MCF))-guest (tungsten polyoxometalate) nanocomposite material: an efficient and reusable catalyst for selective oxidation of sulfides to sulfoxides and sulfones, Catalysis Communications, 29 (2012) 48-52.
[57] R. Gao, X. Yang, W.-L. Dai, Y. Le, H. Li, K. Fan, High-activity, single-site mesoporous WO3-MCF materials for the catalytic epoxidation of cycloocta-1,5-diene with aqueous hydrogen peroxide, Journal of Catalysis, 256 (2008) 259-267.
[58] P. Sharma, S.D. Park, K.T. Park, J.H. Park, C.Y. Jang, S.C. Nam, I.H. Baek, Mesoporous cellular foams supported $Fe_{2.0}SiW_{12}O_{40}$: Synthesis, characterization and application to CO_2 sorption, Powder Technology, 233 (2013) 161-168.
[59] W.-H. Chen, Q. Zhao, H.-P. Lin, Y.-S. Yang, C.-Y. Mou, S.-B. Liu, Hydrocracking in Al-MCM-41: diffusion effect, Microporous and Mesoporous Materials, 66 (2003) 209-218.
[60] K. Szczodrowski, B. Prélot, S. Lantenois, J.-M. Douillard, J. Zajac, Effect of heteroatom doping on surface acidity and hydrophilicity of Al, Ti, Zr-doped mesoporous SBA-15, Microporous and Mesoporous Materials, 124 (2009) 84-93.
[61] G. Muthu Kumaran, S. Garg, K. Soni, M. Kumar, J.K. Gupta, L.D. Sharma, K.S. Rama Rao, G. Murali Dhar, Synthesis and characterization of acidic properties of Al-SBA-15 materials with varying Si/Al ratios, Microporous and Mesoporous Materials, 114 (2008) 103-109.
[62] G.M. Dhar, G.M. Kumaran, M. Kumar, K.S. Rawat, L.D. Sharma, B.D. Raju, K.S.R. Rao, Physico-chemical characterization and catalysis on SBA-15 supported molybdenum hydrotreating catalysts, Catalysis Today, 99 (2005) 309-314.
[63] B. Al Alwan, E. Sari, S.O. Salley, K.Y.S. Ng, Effect of metal ratio and preparation method on nickel-tungsten carbide catalyst for hydrocracking of distillers dried grains with solubles corn oil, Industrial and Engineering Chemistry Research, 53 (2014) 6923-6933.
[64] M. Gómez-Cazalilla, J.M. Mérida-Robles, A. Gurbani, E. Rodríguez-Castellón, A. Jiménez-López, Characterization and acidic properties of Al-SBA-15 materials

prepared by post-synthesis alumination of a low-cost ordered mesoporous silica, Journal of Solid State Chemistry, 180 (2007) 1130-1140.

BIBLIOGRAPHY

Agudelo J.L., B. Mezari, E.J.M. Hensen, S.A. Giraldo, L.J. Hoyos, On the effect of EDTA treatment on the acidic properties of USY zeolite and its performance in vacuum gas oil hydrocracking, Applied Catalysis A: General, 488 (2014) 219-230.

Ali S. Ahmed, M. Elias Biswas, T. Yoneda, T. Miura, H. Hamid, E. Iwamatsu, H. Al-Suaibi, A novel catalyst for heavy oil hydrocracking, in: H. Hideshi, O. Kiyoshi (Eds.) Studies in Surface Science and Catalysis, Elsevier, 1999, pp. 407-410.

Alsobaai A.M., R. Zakaria, B.H. Hameed, Hydrocracking of petroleum gas oil over NiW/MCM-48-USY composite catalyst, Fuel Processing Technology, 88 (2007) 921-928.

Alwan. B. Al, E. Sari, S.O. Salley, K.Y.S. Ng, Effect of metal ratio and preparation method on nickel-tungsten carbide catalyst for hydrocracking of distillers dried grains with solubles corn oil, Industrial and Engineering Chemistry Research, 53 (2014) 6923-6933.

Bellussi. G., G. Rispoli, A. Landoni, R. Millini, D. Molinari, E. Montanari, D. Moscotti, P. Pollesel, Hydroconversion of heavy residues in slurry reactors: Developments and perspectives, Journal of Catalysis, (2013).

Benazzi. E., L. Leite, N. Marchal-George, H. Toulhoat, P. Raybaud, New insights into parameters controlling the selectivity in hydrocracking reactions, Journal of Catalysis, 217 (2003) 376-387.

Blanchard. J., M. Breysse, K. Fajerwerg, C. Louis, C.E. Hédoire, A. Sampieri, S. Zeng, G. Pérot, H. Nie, D. Li, Acidic zeolites and Al-SBA-15 as supports for sulfide phases: application to hydrotreating reactions, in: N.Ž. J. Čejka, P. Nachtigall (Eds.) Studies in Surface Science and Catalysis, Elsevier, 2005, pp. 1517-1524.

Boahene P.E., K.K. Soni, A.K. Dalai, J. Adjaye, Application of different pore diameter SBA-15 supports for heavy gas oil hydrotreatment using FeW catalyst, Applied Catalysis A: General, 402 (2011) 31-40.

Boahene P.E., K.K. Soni, A.K. Dalai, J. Adjaye, Hydroprocessing of heavy gas oils using FeW/SBA-15 catalysts: Experimentals, optimization of metals loading, and kinetics study, Catalysis Today, (2012).

Byambajav E., Hydrocracking of asphaltene with metal catalysts supported on SBA-15, Applied Catalysis A: General, 252 (2003) 193-204.

Byambajav. E., Y. Ohtsuka, Cracking behavior of asphaltene in the presence of iron catalysts supported on mesoporous molecular sieve with different pore diameters, Fuel, 82 (2003) 1571-1577.

Chen. W.-H., Q. Zhao, H.-P. Lin, Y.-S. Yang, C.-Y. Mou, S.-B. Liu, Hydrocracking in Al-MCM-41: diffusion effect, Microporous and Mesoporous Materials, 66 (2003) 209-218.

Contescu. C., J. Jagiello, J.A. Schwarz, Proton affinity distributions: A scientific basis for the design and construction of supported metal catalysts, in: J.M.B.D.P.A.J. G. Poncelet, P. Grange (Eds.) Studies in Surface Science and Catalysis, Elsevier, 1995, pp. 237-252.

Contescu. C., V.T. Popa, J.B. Miller, E.I. Ko, J.A. Schwarz, Proton Affinity Distributions of TiO2-SiO2 and ZrO2-SiO2 Mixed Oxides and Their Relationship to Catalyst Activities for 1-Butene Isomerization, Journal of Catalysis, 157 (1995) 244-258.

Dai. Y. Y.S. Zhou, Q. Wei, Q.Y. Cui, Z. Qin, Influences of Al modification on the properties and catalytic performance of SBA-15 molecular sieves in hydrocracking, Ranliao Huaxue Xuebao/Journal of Fuel Chemistry and Technology, 41 (2013) 1502-1506.

Dhar. G.M., G.M. Kumaran, M. Kumar, K.S. Rawat, L.D. Sharma, B.D. Raju, K.S.R. Rao, Physico-chemical characterization and catalysis on SBA-15 supported molybdenum hydrotreating catalysts, Catalysis Today, 99 (2005) 309-314.

Dragoi. B., E. Dumitriu, S. Bennici, A. Auroux, Acidic and adsorptive properties of Al modified SBA-15 samples, in: P.M. Antoine Gédéon, B. Florence (Eds.) Studies in Surface Science and Catalysis, Elsevier, 2008, pp. 953-956.

Fazaeli. R., H. Aliyan, M.A. Ahmadi, S. Hashemian, Host (aluminum incorporated mesocellulous silica foam (Al-MCF))-guest (tungsten polyoxometalate) nanocomposite material: an efficient and reusable catalyst for selective oxidation of sulfides to sulfoxides and sulfones, Catalysis Communications, 29 (2012) 48-52.

Francis. J., E. Guillon, N. Bats, C. Pichon, A. Corma, L.J. Simon, Design of improved hydrocracking catalysts by increasing the proximity between acid and metallic sites, Applied Catalysis A: General, 409-410 (2011) 140-147.

Franck J.P., J.F. Le page, Catalysts for the Hydrocracking of Heavy Gas Oils into Middle Distillates, in: T. Seiyama, K. Tanabe (Eds.) Studies in Surface Science and Catalysis, Elsevier, 1981, pp. 792-803.

Gao. R., X. Yang, W.-L. Dai, Y. Le, H. Li, K. Fan, High-activity, single-site mesoporous WO3-MCF materials for the catalytic epoxidation of cycloocta-1,5-diene with aqueous hydrogen peroxide, Journal of Catalysis, 256 (2008) 259-267.

Garg . S., K. Soni, G.M. Kumaran, M. Kumar, J.K. Gupta, L.D. Sharma, G.M. Dhar, Effect of Zr-SBA-15 support on catalytic functionalities of Mo, CoMo, NiMo hydrotreating catalysts, Catalysis Today, 130 (2008) 302-308.

Gevert. B.S., J.-E. Otterstedt, Upgrading of directly liquefied biomass to transportation fuels: catalytic cracking, Biomass, 14 (1987) 173-183.

Gómez-Cazalilla. M., A. Infantes-Molina, R. Moreno-Tost, P.J. Maireles-Torres, J. Mérida-Robles, E. Rodríguez-Castellón, A. Jiménez-López, Al-SBA-15 as a support

of catalysts based on chromium sulfide for sulfur removal, Catalysis Today, 143 (2009) 137-144.

Gómez-Cazalilla. M., J.M. Mérida-Robles, A. Gurbani, E. Rodríguez-Castellón, A. Jiménez-López, Characterization and acidic properties of Al-SBA-15 materials prepared by post-synthesis alumination of a low-cost ordered mesoporous silica, Journal of Solid State Chemistry, 180 (2007) 1130-1140.

Hu. W., Q. Luo, Y. Su, L. Chen, Y. Yue, C. Ye, F. Deng, Acid sites in mesoporous Al-SBA-15 material as revealed by solid-state NMR spectroscopy, Microporous and Mesoporous Materials, 92 (2006) 22-30.

Jaroszewska. K., A. Masalska, D. Marek, J.R. Grzechowiak, A. Zemska, Effect of support composition on the activity of Pt and PtMo catalysts in the conversion of n-hexadecane, Catalysis Today, 223 (2014) 76-86.

Jaroszewska. K., A. Masalska, K. Bączkowska, J.R. Grzechowiak, Conversion of decalin and 1-methylnaphthalene over AlSBA-15 supported Pt catalysts, Catalysis Today, 196 (2012) 110-118.

Klimova. T., J. Reyes, O. Gutiérrez, L. Lizama, Novel bifunctional NiMo/Al-SBA-15 catalysts for deep hydrodesulfurization: Effect of support Si/Al ratio, Applied Catalysis A: General, 335 (2008) 159-171.

Klimova. T., M. Calderón, J. Ramírez, Ni and Mo interaction with Al-containing MCM-41 support and its effect on the catalytic behavior in DBT hydrodesulfurization, Applied Catalysis A: General, 240 (2003) 29-40.

Kloprogge. J.T., W.J.J. Welters, E. Booy, V.H.J. de Beer, R.A. van Santen, J.W. Geus, J.B.H. Jansen, Catalytic activity of nickel sulfide catalysts supported on Al-pillared montmorillonite for thiophene hydrodesulfurization, Applied Catalysis A: General, 97 (1993) 77-85.

Knözinger.,H. P. Ratnasamy, Catalytic Aluminas: Surface Models and Characterization of Surface Sites, Catalysis Reviews, 17 (1978) 31-70.

Koekkoek. A.J.J., J.A.R. van Veen, P.B. Gerrtisen, P. Giltay, P.C.M.M. Magusin, E.J.M. Hensen, Brønsted acidity of Al/SBA-15, Microporous and Mesoporous Materials, 151 (2012) 34-43.

Kumaran. G. Muthu, S. Garg, K. Soni, M. Kumar, J.K. Gupta, L.D. Sharma, K.S. Rama Rao, G. Murali Dhar, Synthesis and characterization of acidic properties of Al-SBA-15 materials with varying Si/Al ratios, Microporous and Mesoporous Materials, 114 (2008) 103-109.

Kumaran. G. Muthu, S. Garg, K. Soni, M. Kumar, L.D. Sharma, G. Murali Dhar, K.S. Rama Rao, Effect of Al-SBA-15 support on catalytic functionalities of hydrotreating catalysts: I. Effect of variation of Si/Al ratio on catalytic functionalities, Applied Catalysis A: General, 305 (2006) 123-129.

Lahiri C.R., D. Biswas, High pressure hydrocracking of vacuum gas oil to middle distillates, Physica B+C, 139–140 (1986) 725-728.

Lei. Z., L. Gao, H. Shui, W. Chen, Z. Wang, S. Ren, Hydrotreatment of heavy oil from a direct coal liquefaction process on sulfided Ni–W/SBA-15 catalysts, Fuel Processing Technology, 92 (2011) 2055-2060.

Li. B., J. Xu, X. Li, J. Liu, S. Zuo, Z. Pan, Z. Wu, Bimetallic iron and cobalt incorporated MFI/MCM-41 composite and its catalytic properties, Materials Research Bulletin, 47 (2012) 1142-1148.

Li. Y., D. Pan, C. Yu, Y. Fan, X. Bao, Synthesis and hydrodesulfurization properties of NiW catalyst supported on high-aluminum-content, highly ordered, and hydrothermally stable Al-SBA-15, Journal of Catalysis, 286 (2012) 124-136.

Liang. C., M.-C. Wei, H.-H. Tseng, E.-C. Shu, Synthesis and characterization of the acidic properties and pore texture of Al-SBA-15 supports for the canola oil transesterification, Chemical Engineering Journal, 223 (2013) 785-794.

Lualdi. M., G. Di Carlo, S. Lögdberg, S. Järås, M. Boutonnet, V. La Parola, L.F. Liotta, G.M. Ingo, A.M. Venezia, Effect of Ti and Al addition via direct synthesis to SBA-15 as support for cobalt based Fischer-Tropsch catalysts, Applied Catalysis A: General, 443–444 (2012) 76-86.

Mendoza-Nieto. J.A., I. Puente-Lee, C. Salcedo-Luna, T. Klimova, Effect of titania grafting on behavior of NiMo hydrodesulfurization catalysts supported on different types of silica, Fuel, 100 (2012) 100-109.

Montanari. R.S.D.M., IT), Marchionna, Mario (Milan, IT), Panariti, Nicoletta (Lecco, IT), Delbianco, Alberto (Magenta, IT), Rosi, Sergio (San Donato Milanese, IT) Process for the conversion of heavy feedstocks such as heavy crude oils and distillation residues, in: US Patent 8,017,000, ENI S.p.A. (Rome, IT),SNAMPROGETTI S.p.A. (San Donato Milanese, IT),ENITECNOLOGIE S.p.A. (San Donato Milanese, IT), United States, 2011.

Mouli K. Chandra, K. Soni, A. Dalai, J. Adjaye, Effect of pore diameter of Ni–Mo/Al-SBA-15 catalysts on the hydrotreating of heavy gas oil, Applied Catalysis A: General, 404 (2011) 21-29.

Ortiz-Moreno H., J. Ramírez, F. Sanchez-Minero, R. Cuevas, J. Ancheyta, Hydrocracking of Maya crude oil in a slurry-phase batch reactor. II. Effect of catalyst load, Fuel, 130 (2014) 263-272.

Park. Y.K., H.W. Lee, J.K. Jeon, J. Han, C.U. Kim, S.Y. Jeong, K.E. Jeong, Hydroconversion of n-dodecane over nanoporous catalysts, Journal of Nanoscience and Nanotechnology, 13 (2013) 714-717.

Rouquerol. F., J. Rouquerol, K. Sing Adosrption by Powders and Porous Solids. Principles, Methodology and Applications.

Rouquerol. J., D. Avnir, C.W. Fairbridge, D.H. Everett, J.H. Haynes, N. Pernicone, J.D. Framsay, K. Sing , K.K. Unger, Recommendations for the characterizations of porous solids (Technical Report), Pure & Appl. Chem, 66 (1994) 1739-1758.

Seo. M.G., D.W. Lee, K.Y. Lee, D.J. Moon, Pt/Al-SBA-15 catalysts for hydrocracking of C21-C34 n-paraffin mixture into gasoline and diesel fractions, Fuel, 143 (2015) 63-71.

Sharma. P., S.D. Park, K.T. Park, J.H. Park, C.Y. Jang, S.C. Nam, I.H. Baek, Mesoporous cellular foams supported Fe2.0SiW12O40: Synthesis, characterization and application to CO2 sorption, Powder Technology, 233 (2013) 161-168.

Song. M., C. Zou, G. Niu, D. Zhao, Improving the Hydrothermal Stability of Mesoporous Silica SBA-15 by Pre-treatment with (NH4)2SiF6, Chinese Journal of Catalysis, 33 (2012) 140-151.

Stucky. G.D., B.F. Chmelka, D. Zhao, N. Melosh, Q. Huo, J. Feng, P. Yang, D. Pine, D. Margolese, W. Lukens, Block copolymer processing for mesostructured inorganic oxide materials, in, Google Patents, 2003.

Sun X., H. Fan, J. Zhu, Effect of addition of Y-Al-SBA-15 composite zeolite on catalyst performance in hydrocracking, Shiyou Huagong/Petrochemical Technology, 42 (2013) 518-523.

Szczodrowski. K., B. Prélot, S. Lantenois, J.-M. Douillard, J. Zajac, Effect of heteroatom doping on surface acidity and hydrophilicity of Al, Ti, Zr-doped mesoporous SBA-15, Microporous and Mesoporous Materials, 124 (2009) 84-93.

Villasana. Y., F. Ruscio-Vanalesti, C. Pfaff, F.J. Méndez, M.Á. Luis-Luis, J.L. Brito, Atomic ratio effect on catalytic performance of FeW-based carbides and nitrides on thiophene hydrodesulfurization, Fuel, 110 (2013) 259-267.

Waldron. K., Z. Wu, D. Zhao, X.D. Chen, C. Selomulya, On the improvement of pore accessibility through post-synthesis hydrothermal treatments of spray dried SBA-15 microspheres, Chemical Engineering Science, 127 (2015) 276-284.

Widyaningrum R.N., T.L. Church, M. Zhao, A.T. Harris, Mesocellular-foam-silica-supported Ni catalyst: Effect of pore size on H2 production from cellulose pyrolysis, International Journal of Hydrogen Energy, 37 (2012) 9590-9601.

Yue. Y.H., A. Gédéon, J.L. Bonardet, J.B. d'Espinose, N. Melosh, J. Fraissard, Direct incorporation of Al in SBA mesoporous materials: characterization, stability and catalytic activity, in: S. Abdelhamid, J. Mietek (Eds.) Studies in Surface Science and Catalysis, Elsevier, 2000, pp. 209-218.

Zeng. S., J. Blanchard, M. Breysse, Y. Shi, X. Shu, H. Nie, D. Li, Post-synthesis alumination of SBA-15 in aqueous solution: A versatile tool for the preparation of acidic Al-SBA-15 supports, Microporous and Mesoporous Materials, 85 (2005) 297-304.

Zhang. W.-H., L. Zhang, J. Xiu, Z. Shen, Y. Li, P. Ying, C. Li, Pore size design of ordered mesoporous silicas by controlling micellar properties of triblock copolymer EO20PO70EO20, Microporous and Mesoporous Materials, 89 (2006) 179-185.

Zhang. X., F. Zhang, X. Yan, Z. Zhang, F. Sun, Z. Wang, D. Zhao, Hydrocracking of heavy oil using zeolites Y/Al-SBA-15 composites as catalyst supports, Journal of Porous Materials, 15 (2007) 145-150.

Zhao. D., J. Feng, Q. Huo, N. Melosh, G.H. Fredrickson, B.F. Chmelka, G.D. Stucky, Triblock Copolymer Syntheses of Mesoporous Silica with Periodic 50 to 300 Angstrom Pores, Science, 279 (1998) 548-552.

Zhao. D., Y. Wan, Chapter 8 The synthesis of mesoporous molecular sieves, in: H.v.B.A.C. Jiří Čejka, S. Ferdi (Eds.) Studies in Surface Science and Catalysis, Elsevier, 2007, pp. 241-III.

Zhu. J., J. Wang, X. Sun, J. Yang, Effect of Al-SBA-15 preparation method on the performance of hydrocracking catalyst with Al-SBA-15/USY composite support, Petroleum Processing and Petrochemicals, 43 (2012) 28-32.